arXiv:2001.05543v2 [math.NA] 4 Mar 2021

A parabolic local problem with exponential decay of the resonance error for numerical homogenization

Assyr Abdulle* Doghonay Arjmand† Edoardo Paganoni‡

Abstract

This paper aims at an accurate and efficient computation of effective quantities, e.g., the homogenized coefficients for approximating the solutions to partial differential equations with oscillatory coefficients. Typical multiscale methods are based on a micro-macro coupling, where the macro model describes the coarse scale behaviour, and the micro model is solved only locally to upscale the effective quantities, which are missing in the macro model. The fact that the micro problems are solved over small domains within the entire macroscopic domain, implies imposing artificial boundary conditions on the boundary of the microscopic domains. A naive treatment of these artificial boundary conditions leads to a first order error in ε/δ, where $\varepsilon < \delta$ represents the characteristic length of the small scale oscillations and δ^d is the size of micro domain. This error dominates all other errors originating from the discretization of the macro and the micro problems, and its reduction is a main issue in today's engineering multiscale computations. The objective of the present work is to analyse a parabolic approach, first announced in [A. Abdulle, D. Arjmand, E. Paganoni, C. R. Acad. Sci. Paris, Ser. I, 2019], for computing the homogenized coefficients with arbitrarily high convergence rates in ε/δ. The analysis covers the setting of periodic microstructure, and numerical simulations are provided to verify the theoretical findings for more general settings, e.g. non-periodic micro structures.

Keywords: resonance error, Green's function, effective coefficients, correctors, numerical homogenization

AMS Subject Classification: 35B27, 76M50, 35K20, 65L70

*Institute of Mathematics, École Polytechnique Fédérale de Lausanne, 1015, Station 8, Lausanne, CH-1015, Switzerland, assyr.abdulle@epfl.ch

†Division of Applied Mathematics, School of Education, Culture and Communication, Mälardalen University, Box 883, 721 23, Västerås, Sweden, doghonay.arjmand@mdh.se

‡Institute of Mathematics, École Polytechnique Fédérale de Lausanne, Station 8, Lausanne, CH-1015, Switzerland, edoardo.paga@gmail.com

1 Introduction

Multiscale problems involving several spatial and temporal scales are ubiquitous in physics and engineering. We mention for example, stiff stochastic differential equations (SDEs) in biological and chemical systems, oscillatory physical systems, partial differential equations (PDEs) with multiscale data resonance, e.g., mechanics of composite materials, fracture dynamics of solids, PDEs with oscillating parameters, see Ref. 3,19,30,33,37 and the references therein. A common computational challenge in relation with such multiscale problems is the presence of small scales in the model which should be represented over a much larger macroscopic scale of interest. One rather classical way of overcoming this issue is to analytically derive macroscopic equations from a given microscopic model, and then solve the resulting macroscale equation at a cheaper computational cost. However, such derivations often come together with some simplifying assumptions, making the accuracy of the macroscopic model questionable once the restrictive assumptions are relaxed. In contrast, multiscale numerical methods result in models with improved accuracy and efficiency as they rely on a coupling between microscopic and macroscopic models, combining the efficiency of macroscopic models with the accuracy of microscopic ones. Inexact couplings may afflict such methods by the so-called *resonance error*, Ref. 3,31. Reducing such an error is a common problem of modern multiscale methods designed over the last two decades.

This paper concerns the numerical homogenization of elliptic partial differential equations with multiscale coefficients, whose oscillation length scale (denoted by ε) is much smaller than the size of the domain $\Omega \subset \mathbb{R}^d$, which is bounded and convex. Our model problem is the following ε-indexed family of elliptic equations on Ω

$$\begin{cases} -\nabla \cdot (a^\varepsilon(\mathbf{x}) \nabla u^\varepsilon) = f & \text{in } \Omega \\ u^\varepsilon = 0 & \text{on } \partial\Omega. \end{cases} \tag{1}$$

Here $a^\varepsilon(\mathbf{x}) \in [L^\infty(\Omega)]^{d\times d}$ is symmetric, uniformly elliptic and bounded, i.e., $\exists\, \alpha,\, \beta > 0$ such that

$$\alpha \left|\zeta\right|^2 \leq \zeta \cdot a^\varepsilon(\mathbf{x}) \zeta \leq \beta \left|\zeta\right|^2, \forall \zeta \in \mathbb{R}^d, \text{ a.e. } \mathbf{x} \in \Omega, \forall \varepsilon > 0. \tag{2}$$

The well-posedness of the original problem (1) is then well-known for any $f \in H^{-1}(\Omega)$. As $\varepsilon \to 0$, the solution of (1) can be approximated, by the solution of the so-called homogenized equation:

$$\begin{cases} -\nabla \cdot \left(a^0(\mathbf{x}) \nabla u^0\right) = f & \text{in } \Omega \\ u^0 = 0 & \text{on } \partial\Omega, \end{cases} \tag{3}$$

where the coefficients a^0_{ij} (and hence the solution u^0) no longer oscillate at the ε-scale. By using the concepts of G-convergence for the symmetric case, Ref. 41, one can show that the homogenized problem (3) is the limit for $\varepsilon \to 0$ of

a subsequence of problems (1). In general, we do not have explicit formulae for evaluating the homogenized tensor, unless certain structural assumptions on $a^\varepsilon(\mathbf{x})$ are made. For example, if $a^\varepsilon(\mathbf{x}) = a(\mathbf{x}/\varepsilon)$ is K-periodic, then the homogenized tensor a^0 is given by

$$\mathbf{e}_i \cdot a^0 \mathbf{e}_j = \fint_K \mathbf{e}_i \cdot a(\mathbf{x}) \left(\mathbf{e}_j + \nabla \chi^j(\mathbf{x})\right) \, d\mathbf{x}, \quad i,j = 1,\dots,d, \tag{4}$$

where $K := (-1/2, 1/2)^d$ is the unit cube in $\mathbb{R}^d$, and the functions $\{\chi^i\}_{i=1}^d$ are the solutions of the so-called *cell problems*:

$$\begin{cases} -\nabla \cdot \left(a(\mathbf{x}) \nabla \chi^i\right) = \nabla \cdot \left(a(\mathbf{x}) \mathbf{e}_i\right) & \text{in } K, \\ \chi^i \quad K\text{-periodic.} \end{cases} \tag{5}$$

In (4) and (5) we have used the substitution $\mathbf{y} = \frac{\mathbf{x}}{\varepsilon}$, mapping a sampling domain of size ε^d to the unit cube K. For simplicity of notation, we will again denote by $\mathbf{x}$ (instead of $\mathbf{y}$) the variable on the unit cube. We refer to Ref. 15,18,34 for further technical details.

When the period of the microstructure is not known exactly or the periodicity assumption is relaxed (e.g., if a is random stationary ergodic or quasi-periodic tensor), the formula (4) breaks down. In this case, (4) may be replaced by

$$\mathbf{e}_i \cdot a_R^0 \mathbf{e}_j = \fint_{K_R} \mathbf{e}_i \cdot a(\mathbf{x}) \left(\mathbf{e}_j + \nabla \chi_R^j(\mathbf{x})\right) \, d\mathbf{x}, \quad i,j = 1,\dots,d, \tag{6}$$

where $K_R := (-R/2, R/2)^d$, and[1]

$$\begin{cases} -\nabla \cdot \left(a(\mathbf{x}) \nabla \chi_R^i\right) = \nabla \cdot \left(a(\mathbf{x}) \mathbf{e}_i\right) & \text{in } K_R \\ \chi_R^i(\mathbf{x}) = 0 & \text{on } \partial K_R, \end{cases} \tag{7}$$

and the homogenized coefficient a^0 is given by

$$a^0 = \lim_{R \to \infty} a_R^0.$$

Assume for a moment that the tensor a is K-periodic and that periodic BCs are imposed in (7), then the homogenized tensor a^0 will be equal to a_R^0 only when R is an integer. When R is not an integer, there will be a difference between χ_R and χ on ∂K_R, which results in a so-called resonance error, Ref. 6,20,21[2],

$$e_{MOD} := \left\| a_R^0 - a^0 \right\|_F \leq C \frac{1}{R}, \tag{8}$$

where $\|\cdot\|_F$ denotes the Frobenius norm for a tensor. Note that the first order rate is valid also when the problem (7) is equipped with periodic BCs. From

[1] In (7), the choice of the boundary condition (BC) is not unique, and the homogeneous Dirichlet BCs can be safely replaced e.g., by periodic BCs without any change in (8).

[2] We denote the resonance error by e_{MOD}, as in Ref. 6.

a computational point of view, this first order decay rate of the error is the efficiency and accuracy bottleneck of numerical upscaling schemes, i.e., in order to reduce the resonance error down to practically reasonable accuracies, one needs to solve the problem (7) over large computational domains K_R, possibly on each quadrature point of a macro computational domain (see Ref. 6, 20), which becomes prohibitively expensive. Our central goal is then to design micro models which reduce the resonance error down to desired accuracies without requiring a substantial enlargement of the computational domain K_R. In subsection 1.1, we provide a review of existing strategies, some of which improve the decay rate of the resonance error.

In this work, we restricted ourselves to the analysis of the resonance error for the parabolic local problems under the assumption that the coefficients are periodic and oscillate only at the ε-scale, $a^\varepsilon(\mathbf{x}) = a(\mathbf{x}/\varepsilon)$. The analysis can be extended to the case of locally periodic media, $a^\varepsilon(\mathbf{x}) = a(\mathbf{x}, \mathbf{x}/\varepsilon)$, where the coefficients are ε-periodic in the second argument. In such a case, the parabolic micro problems can still be employed to approximate the homogenized coefficients in the quadrature points of the macro computational domain at the cost of introducing a *collocation* error. Having to fix the first variable of $a(\mathbf{x}, \mathbf{y})$ in the micro model computations produces the new error term. The collocation error has been previously analysed in the context of elliptic cell problems, e.g. in Ref. 4, and similar ideas can be extrapolated to the setting of the present work.

The present work addresses the problem of computing the homogenized limit for a single equation with oscillating coefficients. The techniques used here, in particular the use of the fundamental solution of parabolic equations, are not directly extendable to linear systems, as problems in linear elasticity. Nevertheless, we believe that the ideas presented here can provide a fairly good road-map for generalizing the parabolic approach to such more complex cases.

1.1 Existing approaches for reducing the resonance error

Over the last two decades, several interesting approaches have been proposed to reduce the resonance error. These strategies can be classified in two classes: a) Methods which reduce the prefactor (but not the convergence rate) in (8), b) Methods which improve the convergence rate.

a) Methods reducing the prefactor only:

One of the very first approaches to reduce the prefactor is based on the idea of oversampling, see Ref. 31. In oversampling, the cell problem (7) is solved over K_R, while the computation of the homogenized coefficient takes place in an interior domain $K_L \subset K_R$. Another attempt is based on exploring the combined effect of oversampling and imposing different BCs (Dirichlet, Neumann and periodic) for (7), see Ref. 43. It has been found that the periodic BCs perform better than the other two. Moreover, the Dirichlet BCs tend to overestimate the effective coefficients, while Neumann BCs underestimate them. Clearly, the use of these strategies becomes questionable if one is interested in practically relevant error tolerances, since there is still a need for substantially enlarging

the computational domain K_R before reaching a satisfactory accuracy.

b) Methods improving the convergence rate:

Several methods which rely on modifying the cell problem (7), while still retaining a good approximation (with higher order convergence rates in $1/R$) of the homogenized coefficient have been developed in the last few years. In Ref. 16, an approach with weight (filtering) functions in the very definition of the cell problem, as well as in the averaging formula, is proposed. While the method has arbitrarily high convergence rates in a one-dimensional setting, the convergence rate in dimensions $d > 1$ has been proved to be 2. Numerical simulations demonstrate the optimality of the second order rate in dimension $d > 1$.

Another promising strategyis to add a small zero-th order regularization term to the cell problem (7) so as to make the associated Green's function exponentially decaying. This idea was originally introduced in the context of stochastic homogenization Ref. 28, 29, and an analysis of the boundary error in the periodic case can be found in Ref. 24. The effect of the boundary mismatch will then decay exponentially fast in the interior of $K_L \subset K_R$. However, the method will suffer from a bias (or systematic error) due to added regularization term, which limits the convergence rate to fourth order. Moreover, numerical simulations in Ref. 24 show that the method requires very large values of R to achieve the optimal fourth order asymptotic rate. In Ref. 25, 26, Richardson extrapolation is used to increase the convergence rate to higher orders at the expense of solving the cell problem several times with different regularization terms.

An interesting idea, proposed in Ref. 9, 12, is to solve a second order wave equation on $K_R \times (0, T)$, instead of the elliptic cell problem (7), see also Ref. 11 for an analysis in locally-periodic media. Thanks to the finite speed of propagation of waves, this approach leads to an ultimate removal of the error due to inaccurate BCs if K_R is sufficiently large; i.e., the boundary values will not be seen in an interior region K_L (where the averaging takes place) if $R > L + \sqrt{\|a\|_\infty} T$. Hence, size of the computational domain should increase linearly with respect to the wave speed $\sqrt{\|a\|_\infty}$, which increases also the computational cost. Moreover, solving a wave equation is computationally more challenging than solving an elliptic PDE since an accurate discretization requires a more refined resolution per wave-length, implying a more refined stepsize for temporal discretization due to the presence of CFL condition in typical time-stepping methods for the wave equation such as the leap frog scheme.

The goal of this paper is to provide a rigorous analysis of yet another approach, announced in Ref. 5, based on parabolic cell problems which results in arbitrarily high convergence rates in $1/R$. The parabolic approach adopted here is inspired by Ref. 38 (although the idea of describing corrector functions by means of semigroup was also discussed in Ref. 27) and can be classified under category b), but with significant advantages from a computational point of view in comparison to the above mentioned strategies (see the discussions in the numerical results section). Moreover, this approach can be directly used in

typical upscaling based multiscale formalisms such as the Heterogeneous Multiscale Methods (HMM) Ref. 2, 6, 8, 20, and the equation free approaches Ref. 35, as well as Multiscale Finite Elements Methods (MsFEM) Ref. 31, 32, which are used to approximate either the homogenized solutions to (1) or directly approximating the oscillatory response u^ε in (1).

The paper in structured as follows: in Section 2 we collect our notations and provide some definitions that will be used to present a new approximation scheme for the homogenized tensor. The main results of the present work are reported in Section 3. Section 4 is devoted to the analysis of the modelling error, where arbitrary high order convergence rates are proved. In Section 5, numerical examples are given to verify our theoretical findings. Finally, in Section 6 the computational cost of the parabolic method is analysed theoretically and compared to the classical elliptic scheme.

2 Notations and definitions

We will use the following notations throughout the exposition:

- The Sobolev space $W^{k,p}(\Omega)$ is defined as

  $$W^{k,p}(\Omega) := \{f : D^\gamma f \in L^p(\Omega) \text{ for all multi-index } \gamma \text{ with } |\gamma| \leq k\}.$$

  The norm of a function $f \in W^{k,p}(\Omega)$ is given by

  $$\|f\|_{W^{k,p}(\Omega)} := \begin{cases} \left(\sum_{|\gamma|\leq k} \int_\Omega |D^\gamma f(\mathbf{x})|^p \, d\mathbf{x}\right)^{1/p} & (1 \leq p < \infty) \\ \sum_{|\gamma|\leq k} \text{ess sup}_\Omega |D^\gamma f| & (p = \infty). \end{cases}$$

- The space $W_0^{1,p}(\Omega)$ is the closure in the $W^{1,p}$-norm of $C_c^\infty(\Omega)$, the space of infinitely differentiable functions with compact support in Ω. The norm associated with $W_0^{1,p}(\Omega)$ is

  $$\|f\|^p_{W_0^{1,p}(\Omega)} := \|f\|^p_{L^p(\Omega)} + \|\nabla f\|^p_{L^p(\Omega)}.$$

- The space $W_0^{1,2}(\Omega)$ is also denoted as $H_0^1(\Omega)$. By making use of the Poincaré inequality, the norm

  $$\|f\|_{H_0^1(\Omega)} := \|\nabla f\|_{L^2(\Omega)}$$

  is equivalent to $\|f\|^p_{W_0^{1,2}(\Omega)}$. We will sometimes use this form for the H_0^1-norm.

- We use the notation $\langle f, g\rangle_{L^2(\Omega)} := \int_\Omega fg \, d\mathbf{x}$ to denote the L^2 inner product over Ω.

- The space H_{div} is

$$H_{div}(\Omega) := \{f : f \in [L^2(\Omega)]^d \text{ and } \nabla \cdot f \in L^2(\Omega)\}.$$

  The norm associated with H_{div} is

$$\|f\|^2_{H_{div}(\Omega)} := \|f\|^2_{L^2(\Omega)} + \|\nabla \cdot f\|^2_{L^2(\Omega)}.$$

- The space $W^1_{per}(K)$ is defined as the closure of

$$\left\{ f \in C^\infty_{per}(K) : \int_K f \, d\mathbf{x} = 0 \right\}$$

  for the H^1-norm. Thanks to the Poincaré-Wirtinger inequality, an equivalent norm in $W^1_{per}(K)$ is

$$\|f\|_{W^1_{per(K)}} = \|\nabla f\|_{L^2(K)}.$$

- The space $L^2_0(K)$ is defined as

$$L^2_0(K) = \left\{ f \in L^2(K) : \int_K f \, d\mathbf{x} = 0 \right\}.$$

  It is an Hilbert space with respect to the L^2-inner product.

- Let f belong to the Bochner space $L^p(0,T;X)$, where X is a Banach space. Then the norm associated with this space is defined as

$$\|f\|_{L^p(0,T;X)} := \left(\int_0^T \|f\|^p_X \, dt \right)^{\frac{1}{p}}.$$

- Cubes in $\mathbb{R}^d$ are denoted by $K_L := (-L/2, L/2)^d$. In particular, K is the unit cube $(-1/2, 1/2)^d$.

- By writing C, we mean a generic constant independent of R, L, T which may change in every subsequent occurrence.

- Boldface letters are to distinguish functions in multi-dimensions, e.g., $f(\mathbf{x})$ is to mean a function of several variable ($\mathbf{x} \in \mathbb{R}^d, d \geq 2$), while $f(x)$ will be a function of one variable ($x \in \mathbb{R}$).

- We will use the notation $⨍_D f(\mathbf{x}) \, d\mathbf{x}$ to denote the average $\frac{1}{|D|} \int_D f(\mathbf{x}) \, d\mathbf{x}$ over a domain D.

An important ingredient of the proposed numerical homogenization method are q-th order filter functions introduced in Ref. 24 and defined below.

Definition 2.1 (Definition 3.1 in Ref. 24)**.** *We say that a function $\mu : [-1/2, 1/2] \to \mathbb{R}^+$ belongs to the space $\mathbb{K}^q$ with $q > 0$ if*

i) $\mu \in C^q([-1/2,1/2]) \cap W^{q+1,\infty}((-1/2,1/2))$

ii) $\int_{-1/2}^{1/2} \mu(x)\, dx = 1$,

iii) $\mu^k(-1/2) = \mu^k(1/2) = 0$ *for all* $k \in \{0,\dots,q-1\}$.

In multi-dimensions a q-th order filter $\mu_L : K_L \to \mathbb{R}^+$ *with* $L > 0$ *is defined by*

$$\mu_L(\mathbf{x}) := L^{-d} \prod_{i=1}^{d} \mu\left(\frac{x_i}{L}\right),$$

where μ *is a one dimensional q-th order filter and* $\mathbf{x} = (x_1, x_2, \dots, x_d) \in \mathbb{R}^d$. *In this case, we will say that* $\mu_L \in \mathbb{K}^q(K_L)$. *Note that filters* μ_L *are considered extended to 0 outside of* K_L.

Filters have the property of approximating the average of periodic functions with arbitrary rate of accuracy, as stated in the following lemma (see Ref. 24 for a proof).

Lemma 2.1 (Lemma 3.1 in Ref. 24)**.** *Let* $\mu_L \in \mathbb{K}^q(K_L)$. *Then, for any* K*-periodic function* $f \in L^p(K)$ *with* $1 < p \le 2$, *we have*

$$\left| \int_{K_L} f(\mathbf{x}) \mu_L(\mathbf{x})\, d\mathbf{x} - \fint_K f(\mathbf{x})\, d\mathbf{x} \right| \le C \left\| f \right\|_{L^p(K)} L^{-(q+1)},$$

where C *is a constant independent of* L.

Remark 2.1. *The constant* C *in the above Lemma* 2.1 *depends on the Lipschitz constant of* $\mu^{(q)}$. *The result of Lemma* 2.1 *was proved in Ref. 24 for* K*-periodic* $f \in L^2(K)$ *and, then, extended to the case* $f \in L^p(K)$, $1 < p < 2$.

Definition 2.2. *We say that* $a \in \mathcal{M}(\alpha, \beta, \Omega)$ *if* $a_{ij} = a_{ji}$, $a \in [L^\infty(\Omega)]^{d\times d}$ *and there are constants* $0 < \alpha \le \beta$ *such that*

$$\alpha|\zeta|^2 \le \zeta \cdot a(\mathbf{x})\zeta \le \beta|\zeta|^2, \quad \text{for a.e.} \quad \mathbf{x} \in \Omega, \forall \zeta \in \mathbb{R}^d.$$

We write $a \in \mathcal{M}_{per}(\alpha, \beta, \Omega)$ *if in addition* a *is a* Ω*-periodic function.*

Throughout the exposition, we assume that u^i and v^i, $i = 1, \dots, d$, are the solutions of the following problems:

$$\begin{cases} \dfrac{\partial u^i}{\partial t} - \nabla \cdot (a(\mathbf{x}) \nabla u^i) = 0 & \text{in } K_R \times (0, +\infty) \\ u^i = 0 & \text{on } \partial K_R \times (0, +\infty) \\ u^i(\mathbf{x}, 0) = \nabla \cdot (a(\mathbf{x}) \mathbf{e}_i) & \text{in } K_R, \end{cases} \tag{9}$$

and

$$\begin{cases} \dfrac{\partial v^i}{\partial t} - \nabla \cdot (a(\mathbf{x}) \nabla v^i) = 0 & \text{in } K \times (0, +\infty) \\ v^i(\cdot, t) \quad K\text{-periodic}, \forall t \ge 0 & \\ v^i(\mathbf{x}, 0) = \nabla \cdot (a(\mathbf{x}) \mathbf{e}_i) & \text{in } K. \end{cases} \tag{10}$$

The well-posedness of (9) and (10) are well-known (see, e.g., Ref. 36), and are summarized below.

Proposition 2.1. *Let $a \in \mathcal{M}(\alpha, \beta, K_R)$ and $a(\mathbf{x})\mathbf{e}_i \in H_{div}(K_R)$. Then, (9) has a unique weak solution u^i such that*

$$u^i \in L^2([0,+\infty), H_0^1(K_R)), \partial_t u^i \in L^2([0,+\infty), H^{-1}(K_R)).$$

It follows that $u^i \in C([0,+\infty), L^2(K_R))$, and there exists a constant $C > 0$ such that the following bound holds true:

$$\left\|u^i\right\|_{L^\infty([0,+\infty),L^2(K_R))} + \left\|u^i\right\|_{L^2\left([0,+\infty),H_0^1(K_R)\right)} \leq C \left\|\nabla \cdot (a(\mathbf{x})\mathbf{e}_i)\right\|_{L^2(K_R)}.$$

Proposition 2.2. *Let $a \in \mathcal{M}_{per}(\alpha, \beta, K)$ and $a(\mathbf{x})\mathbf{e}_i \in H_{div}(K_R)$. Then, (10) has a unique weak solution v^i such that*

$$v^i \in L^2([0,+\infty), W_{per}^1(K)), \partial_t v^i \in L^2([0,+\infty), W_{per}^1(K)').$$

It follows that $v^i \in C([0,+\infty), L_0^2(K))$, and there exist constants $C > 0$ such that the following bounds hold true:

$$\left\|v^i\right\|_{L^\infty([0,+\infty),L^2(K))} + \left\|v^i\right\|_{L^2\left([0,+\infty),W_{per}^1(K)\right)} \leq C \left\|\nabla \cdot (a(\mathbf{x})\mathbf{e}_i)\right\|_{L^2(K)}.$$

Here, the space $W_{per}^1(K)'$ is the dual space of $W_{per}^1(K)$ (a characterization of this space can be found in Ref. 18). With a slight abuse of notation, in the coming sections the functions v^i will indicate both the solution of (10) on the cell K and its periodic extension to the whole $\mathbb{R}^d$. Finally, we define the bilinear form $B : W_{per}^1(K) \times W_{per}^1(K) \mapsto \mathbb{R}$ through the formula

$$B[u,v] = \int_K \nabla u \cdot a(\mathbf{x}) \nabla v \, d\mathbf{x}. \tag{11}$$

If $a \in \mathcal{M}_{\text{per}}(\alpha, \beta, K)$, the bilinear form $B[\cdot,\cdot]$ is continuous and coercive and there exists a non-decreasing sequence of strictly positive eigenvalues $\{\lambda_j\}_{j=0}^\infty$ and a L^2-orthonormal set of eigenfunctions $\{\varphi_j\}_{j=0}^\infty \subset W_{per}^1(K)$ such that

$$B[\varphi_j, w] = \lambda_j \langle \varphi_j, w \rangle_{L^2(K)}, \quad \forall w \in W_{per}^1(K). \tag{12}$$

3 Main results

The starting point of the analysis is the following new formula for the approximation of the homogenized coefficient a^0 in (3)

$$\mathbf{e}_i a_{R,L,T}^0 \mathbf{e}_j = \int_{K_L} \mathbf{e}_i \cdot a(\mathbf{x}) \mathbf{e}_j \mu_L(\mathbf{x}) \, d\mathbf{x} - 2 \int_0^T \int_{K_L} u^i(\mathbf{x},t) u^j(\mathbf{x},t) \mu_L(\mathbf{x}) \, d\mathbf{x} \, dt, \tag{13}$$

where $\{u^i\}_{i=1}^d$ are the solutions of the parabolic problems (9). Note that the parabolic solutions $\{u^i\}_{i=1}^d$ are solved over K_R, from which it follows the dependency of $a^0_{R,L,T}$ on the parameter R, while the averaging is taking place over the domain $K_L \subset K_R$. The aim of this section is two-fold: first, in Subsection 3.1, we will recall a result which is proved in Ref. 5, where the equivalence between the approximate homogenized coefficient (13) (when $T = \infty$, $L = R$ and the constant filter $\mu_L = L^{-d}$ is adopted), and the approximation (6) based on elliptic cell problems (when χ^i_R is supplied with homogeneous Dirichlet BCs) is shown. Next, in Subsection 3.2, we will present our main statement in Theorem 3.2, which states that if T and L are chosen optimally, then we obtain arbitrarily high convergence rates for the difference between $a^0_{R,L,T}$ in (13) and the exact homogenized coefficient a^0 in (4), when $a \in \mathcal{M}_{\rm per}(\alpha, \beta, K)$.

The periodicity of the coefficient a is assumed only to simplify the theory. The method itself can be easily generalized to cases when the homogenized coefficient a^0 is not a constant by shifting the local spatial domains in (13), as well as the parabolic problem (9) to $\mathbf{x} + K_R$, where $\mathbf{x}$ is a point at which the homogenized coefficient a^0_R needs to be computed. One typical example is when the coefficient $a^\varepsilon(\mathbf{x})$ is locally periodic and has both fast and slow variations. In this case, it is even possible to generalize the analysis by considering a local Taylor's expansion of the parabolic solutions (13) around the slow variable following the ideas in Ref. 10.

3.1 Equivalence between the standard and parabolic homogenized coefficients

Assume that the elliptic solutions χ^i_R in (7) are supplied either with periodic or homogeneous Dirichlet BCs. By symmetry of $a(\mathbf{x})$, we can rewrite (6) as:

$$\mathbf{e}_i \cdot a^0_R \mathbf{e}_j = \fint_{K_R} \mathbf{e}_i \cdot a(\mathbf{x}) \mathbf{e}_j \, d\mathbf{x} - \fint_{K_R} \nabla \chi^i_R(\mathbf{x}) \cdot a(\mathbf{x}) \nabla \chi^j_R(\mathbf{x}) \, d\mathbf{x}. \tag{14}$$

Theorem 3.1 provides an alternative expression for the second integral, which will be referred to as the *correction part* of the homogenized tensor, based on the use of parabolic problems over infinite time domain. We refer to Ref. 5 for a rigorous proof.

Theorem 3.1. *Let $a(\mathbf{x}) \in \mathcal{M}(\alpha, \beta, K_R)$, $u^i \in C([0, +\infty), L^2(K_R))$ be the weak solution of (9) and $\chi^i_R \in H^1_0(K_R)$ be the weak solution of (7). Then, for $1 \le i, j \le d$, the following identities hold*

$$\chi^i_R = \int_0^{+\infty} u^i(\cdot, t) \, dt \quad \text{in } H^1_0(K_R), \tag{15}$$

$$\frac{1}{2} \int_{K_R} \nabla \chi^i_R(\mathbf{x}) \cdot a(\mathbf{x}) \nabla \chi^j_R(\mathbf{x}) d\mathbf{x} = \int_0^{+\infty} \int_{K_R} u^i(\mathbf{x}, t) u^j(\mathbf{x}, t) d\mathbf{x} \, dt. \tag{16}$$

Theorem 3.1 implies that if $T = \infty$ (and $\mu_L = L^{-d}$ in K_L with $R = L$) in (13), then the parabolic formulation does not lead to any gain in the first order

convergence rate in (8) due to the equivalence relation above. It is important to notice that we do not need the periodicity assumption on the tensor a for deriving the equivalence. Moreover, the same result holds true if we substitute the homogeneous Dirichlet condition with the periodic boundary conditions, under the periodicity assumption for the tensor a. Then we have the following corollary:

Corollary 3.1. *Let $a(\mathbf{x}) \in \mathcal{M}_{per}(\alpha, \beta, K)$. Let $v^i \in C([0, +\infty), L^2_{per}(K))$ solve* (10)*. Then*

$$\mathbf{e}_i a^0 \mathbf{e}_j = \fint_K \mathbf{e}_i \cdot a(\mathbf{x}) \mathbf{e}_j \, d\mathbf{x} - 2 \int_0^{+\infty} \fint_K v^i(\mathbf{x}, t) v^j(\mathbf{x}, t) \, d\mathbf{x} \, dt. \tag{17}$$

Remark 3.1. *Identities* (14)*,* (16)*, and* (17) *are based on the assumption of symmetry for the matrix $a(\cdot)$. By consequence,* (13) *should be modified for problems with non-symmetric coefficients.*

3.2 Main result: exponential decay of the resonance error

As stated in the Subsection 3.1, the consequence of the equivalence between the parabolic model and the standard elliptic model is that the first order convergence rate of the resonance error in (8) remains unchanged. In this subsection, we summarize our main result which states that we are able to achieve arbitrarily high convergence rates for the resonance error

$$e_{MOD} := \left\| a^0_{R,L,T} - a^0 \right\|_F,$$

upon choosing the parameters T and L optimally. Our basic assumptions, for our main theorem, are the following:

$$a(\cdot) \in \mathcal{M}_{\text{per}}(\alpha, \beta, K), \tag{18a}$$

$$a(\cdot)\mathbf{e}_i \in W^{1,\infty}(K_R), \quad \text{for } i = 1, \ldots, d, \tag{18b}$$

$$v^i \in L^p\left((0,T), W^{1,p}_{per}(K)\right), \quad \text{for } i = 1, \ldots, d, \tag{18c}$$

with $p > p_0 = \max\left\{\frac{d+2}{2}, 2\right\}$.

Remark 3.2. *Let us briefly comment on assumption* (18c)*. This assumption is needed to have sufficient regularity of a boundary layer function defined in* (28)*. One can notice that, for $d = 1$ the classical estimate of $v^i \in L^2\left((0,T), W^{1,2}_{per}(K)\right)$ is sufficient, for $d = 2$ we need $p > 2$ and for $d = 3$ we need $p > 5/2$. The last two conditions are only slightly more restrictive than what we already know on v^i, namely $v^i \in L^2\left((0,T), W^{1,2}_{per}(K)\right)$. Finally, such L^p estimates have been proved (for parabolic problems with homogeneous Dirichlet BCs, as in* (9)*) in Chapter 2, Theorem 2.5 Ref. 15 under appropriate assumptions on $a(\cdot)$, but without an explicit characterization of $p > 2$.*[3]

[3]The assumption $a(\cdot) \in W^{2,p}(K_R)$ is sufficient but might not be necessary, see 15.

Theorem 3.2. *Under assumptions* (18)*, let* $K_R \subset \mathbb{R}^d$ *for* $R \geq 1$*. Let* $a^0_{R,L,T}$ *and* a^0 *be defined, respectively, as in* (13) *and* (4)*, with* u^i *satisfying* (9) *for any* $i = 1, \ldots, d$ *and* $\mu_L \in \mathbb{K}^q(K_L)$*, with* $0 < L < R - 2$*. There exist constants* $\nu(\beta, d) > 0$*,* $0 < c \leq \nu$*,* $\lambda_0(\alpha, d) > 0$*,* $C(\alpha, \beta, d) > 0$ *and* $\tilde{C}_{2,c}(\alpha, \beta, d) > 0$ *such that, if* $T < \frac{2\nu}{d}\left|\tilde{R} - L\right|^2$ *and* $T < \tilde{C}_{2,c}\,|R - L|$*, then*

$$\left\|a^0_{R,L,T} - a^0\right\|_F \leq C\left[L^{-(q+1)} + e^{-2\lambda_0 T} + \frac{R^{d-1}}{T^{d/2}} e^{-c\frac{|R-L|^2}{T}} + \frac{R^{2(d-1)}}{T^d} e^{-2c\frac{|R-L|^2}{T}}\right]. \tag{19}$$

The choice

$$L = k_o R, \quad T = k_T(R - L),$$

with $0 < k_o < 1$ *and* $k_T = \sqrt{\frac{c}{2\lambda_0}}$ *results in the following convergence rate in terms of* R

$$\left\|a^0_{R,L,T} - a^0\right\|_F \leq C\left[R^{-(q+1)} + e^{-\sqrt{2\lambda_0 c}(1-k_o)R}\right], \tag{20}$$

for a constant $C > 0$ *independent of* R*,* L *or* T*.*

3.2.1 Choice of the parameters

The choice of T has a direct influence on the decay of the exponential part of the error. If k_T is too small then the first exponential term in (19) will be dominant, while if k_T is too large then the last two exponentials will dominate the error bound (provided that R and L are not extremely large). The optimal value of k_T depends on λ_0 and c, but their values are not available in most of the cases. A practical choice of k_T can be made by using approximate values for c and λ_0. The constant c, which appears in the last two exponential terms in (19), can be taken arbitrarily close to the constant ν in the exponent of the Nash–Aronson estimate (30), where the constant ν depends only on the dimension d and the constant β in Definition 2.2 (see Remark 4.2). For λ_0, which is the smallest eigenvalue of the bilinear form (11), the following approximation hold: $\lambda_0 \approx \frac{\pi^2 \alpha}{diam(K)^2} \approx \frac{\pi^2}{d} \inf_{x \in \mathbb{R}^d, i, j} |a_{ij}(x)|$ (see Remark 4.1). As a consequence, the exponent in the exponential term $\sqrt{2\lambda_0 c} \approx \sqrt{\alpha/\beta}$ will depend on the contrast ratio. Later in the analysis, it will be clear that the main idea of limiting $T = \mathcal{O}(R - L)$ is to exploit the mild dependence of the parabolic solutions u^i on the boundary conditions, which is the case if parabolic solutions are evolved over a sufficiently short time. Second, the use of filtering functions μ_L is to achieve high order convergence rates for the averages of oscillatory functions, which is another essential component in achieving high order rates for the resonance error.

4 Error analysis

In this section we prove the bound stated in Theorem 3.2. The proof can be outlined as follows:

Step 1: We exploit the fact that the exact homogenized coefficient a^0 in (4) is equal to (17), and we decompose the error into four terms

$$\begin{aligned}\mathbf{e}_i(a^0_{R,L,T}-a^0)\mathbf{e}_j = &\underbrace{\int_{K_L}\mathbf{e}_i\cdot a(\mathbf{x})\mathbf{e}_j\mu_L(\mathbf{x})\,d\mathbf{x}-\fint_K \mathbf{e}_i\cdot a(\mathbf{x})\mathbf{e}_j\,d\mathbf{x}}_{I^1_{ij}}\\ &\underbrace{+2\int_0^T\int_{K_L} v^i(\mathbf{x},t)v^j(\mathbf{x},t)\mu_L(\mathbf{x})d\mathbf{x}\,dt-2\int_0^T\int_{K_L}u^i(\mathbf{x},t)u^j(\mathbf{x},t)\mu_L(\mathbf{x})d\mathbf{x}\,dt}_{I^2_{ij}}\\ &\underbrace{+2\int_0^T\fint_K v^i(\mathbf{x},t)v^j(\mathbf{x},t)d\mathbf{x}\,dt-2\int_0^T\int_{K_L}v^i(\mathbf{x},t)v^j(\mathbf{x},t)\mu_L(\mathbf{x})d\mathbf{x}\,dt}_{I^3_{ij}}\\ &\underbrace{+2\int_0^{+\infty}\fint_K v^i(\mathbf{x},t)v^j(\mathbf{x},t)d\mathbf{x}\,dt-2\int_0^T\fint_K v^i(\mathbf{x},t)v^j(\mathbf{x},t)d\mathbf{x}\,dt}_{I^4_{ij}}. \quad (21)\end{aligned}$$

Step 2: Estimation of the *averaging* errors I^1_{ij} and I^3_{ij} by means of Lemma 2.1.

Step 3: Estimation of the *truncation* error I^4_{ij} by means of the exponential decrease in time of $\left\|v^i(\cdot,t)\right\|_{L^2(Y)}$.

Step 4: Estimation of the *boundary* error I^2_{ij} by means of upper bounds for the fundamental solution of the parabolic problem and integration over finite time intervals $[0,T]$.

The coming subsections will be devoted to the derivation of upper bounds for I^1_{ij}, I^2_{ij}, I^3_{ij} and I^4_{ij}.

4.1 Bounds for I^1_{ij} and I^3_{ij}

The two error terms studied in this subsection originate from the fact that we are approximating the averages of periodic functions by a weighted average over a bounded domain. For such a reason, these errors will be referred to as *averaging* error for a (I^1_{ij}) and for v^iv^j (I^3_{ij}). The Corollary 4.1 is a direct consequence of Lemma 2.1, and therefore the proof is omitted.

Corollary 4.1. *Let $a\in\mathcal{M}_{per}(\alpha,\beta,K)$ be periodically extended over K_L. Then, there exists $C_1>0$, independent of L, such that*

$$\left|I^1_{ij}\right|\le C_1L^{-(q+1)},\quad i,j=1,\dots,d.$$

Lemma 4.1. *Let $a(\cdot)$ satisfy assumption* (18a)*, let $v^i \in L^2([0,+\infty), W^1_{per}(K))$ be the K-periodic solution of* (10) *and $\mu_L \in \mathbb{K}^q(K_L)$. Then, there exists $C_3 > 0$, independent of L, such that*

$$\left|I^3_{ij}\right| \leq C_3 L^{-(q+1)}.$$

Proof. By applying Lemma 2.1 to function $2v^iv^j$ we get:

$$\left|I^3_{ij}\right| \leq \int_0^T C \left\|v^i(\cdot,t)v^j(\cdot,t)\right\|_{L^p(K)} L^{-(q+1)}\, dt, \tag{22}$$

with $1 < p \leq 2$. Following the proof of Lemma 2.1 (see Appendix A, Ref. 24), we deduce that, for any $q \geq 2$ one can also choose $p = 1$ in the inequality above. Therefore, by the use of Cauchy–Schwarz and Hölder inequalities, I^3_{ij} can be estimated as

$$\begin{aligned}
\left|I^3_{ij}\right| &\leq \int_0^T C \left\|v^i(\cdot,t)v^j(\cdot,t)\right\|_{L^1(K)} L^{-(q+1)}\, dt \\
&\leq CL^{-(q+1)} \int_0^T \left\|v^i(\cdot,t)\right\|_{L^2(K)} \left\|v^j(\cdot,t)\right\|_{L^2(K)}\, dt \\
&\leq CL^{-(q+1)} \left\|v^i\right\|_{L^2([0,+\infty),L^2(K))} \left\|v^j\right\|_{L^2([0,+\infty),L^2(K))}.
\end{aligned}$$

The result follows by choosing

$$C_3 := C \left\|v^i\right\|_{L^2([0,+\infty),L^2(K))} \left\|v^j\right\|_{L^2([0,+\infty),L^2(K))}.$$

In the case $q \in \{0,1\}$ we cannot utilize any more the L^1-norm of the product. In view of (22), with the choice $p = 3/2$, it follows that

$$\begin{aligned}
\left|I^3_{ij}\right| &\leq \int_0^T C \left\|v^i(\cdot,t)v^j(\cdot,t)\right\|_{L^{3/2}(K)} L^{-(q+1)}\, dt \\
&\leq \int_0^T C \left\|v^i(\cdot,t)v^j(\cdot,t)\right\|_{W^{1,1}(K)} L^{-(q+1)}\, dt \\
&\leq \int_0^T C \left\|v^i(\cdot,t)\right\|_{W^1_{per}(K)} \left\|v^j(\cdot,t)\right\|_{W^1_{per}(K)} L^{-(q+1)}\, dt \\
&\leq CL^{-(q+1)} \left\|v^i\right\|_{L^2([0,+\infty),W^1_{per}(K))} \left\|v^j\right\|_{L^2([0,+\infty),W^1_{per}(K))},
\end{aligned}$$

where the first inequality is a direct application of Lemma 2.1, the second inequality follows from the continuous inclusion of $W^{1,1}(K)$ in $L^{3/2}(K)$, the third inequality comes from the embedding $W^1_{per}(K) \subset W^{1,1}(K)$ and the validity of the derivative product rule for functions $v^i \in W^{1,p}(\Omega) \cap L^\infty(\Omega)$ for $1 \leq p \leq \infty$ (see, e.g. Ref. 17 for a proof) which implies:

$$\left\|v^i(\cdot,t)v^j(\cdot,t)\right\|_{W^{1,1}(K)} \leq C \left\|v^i(\cdot,t)\right\|_{W^1_{per}(K)} \left\|v^j(\cdot,t)\right\|_{W^1_{per}(K)}.$$

Finally, the last inequality is the Chauchy-Schwarz inequality. The result follows by choosing

$$C_3 := C \left\|v^i\right\|_{L^2([0,+\infty),W^1_{per}(K))} \left\|v^j\right\|_{L^2([0,+\infty),W^1_{per}(K))}.$$

□

4.2 Bound for I^4_{ij}

In this subsection we derive an *a-priori* estimate for the truncation error, which originates from the restriction of the time integral in (13) on the finite interval $[0,T]$. As it will be clearer from the coming analysis, the time truncation is essential for improving the convergence rate of the resonance error, as large values of T result in a pollution of the correctors. First of all, we recall the following lemma on the exponential decay in time of $\left\|v^i(\cdot,t)\right\|_{L^2(K)}$.

Lemma 4.2. *Let $v^i \in C([0,\infty), L^2(K))$ be the solution of (10) and let $\lambda_0 > 0$ be the smallest eigenvalue of the bilinear form B introduced in (11). Then*

$$\left\|v^i(\cdot,t)\right\|_{L^2(K)} \leq e^{-\lambda_0 t} \left\|v^i(\cdot,0)\right\|_{L^2(K)}, \quad \text{a. e. } t \in [0,+\infty).$$

Proof. The weak formulation of (10) reads: Find $v^i \in L^2([0,+\infty), W^1_{per}(K))$, $\partial_t v^i \in L^2([0,+\infty), W^1_{per}(K)')$ such that

$$\begin{aligned} &\left(\partial_t v^i, w\right) + B[v^i, w] = 0, \qquad \forall w \in W^1_{per}(K), \\ &v^i(\cdot,0) = \nabla\cdot(a\mathbf{e}_i) \in L^2_0(K). \end{aligned}$$

By using $w = v^i(\cdot,t)$, the second line becomes

$$\frac{1}{2}\frac{d}{dt}\left\|v^i\right\|^2_{L^2(K)} = -B[v^i, v^i].$$

Let $\{\lambda_j\}_{j=0}$ and $\{\varphi_j\}_{j=0}$ be, respectively, the eigenvalues and eigenfunctions of B and let us denote $\hat{v}^i_j := \langle v^i, \varphi_j\rangle_{L^2(K)}$. By orthogonality of the eigenfunctions and Parseval's identity, it holds

$$B[v^i, v^i] = \sum_{j=0}^{\infty} \lambda_j \left|\hat{v}^i_j\right|^2 \geq \lambda_0 \sum_{j=0}^{\infty} \left|\hat{v}^i_j\right|^2 = \lambda_0 \left\|v^i\right\|^2_{L^2(K)}.$$

Then, by coercivity of the bilinear form B and use of the above inequality, we get

$$\left\|v^i\right\|_{L^2(K)} \frac{d}{dt}\left\|v^i\right\|_{L^2(K)} = \frac{1}{2}\frac{d}{dt}\left\|v^i\right\|^2_{L^2(K)} = -B[v^i, v^i] \leq -\lambda_0 \left\|v^i\right\|^2_{L^2(K)}.$$

So, the following differential inequality is derived:

$$\frac{d}{dt}\left\|v^i\right\|_{L^2(K)} \leq -\lambda_0 \left\|v^i\right\|_{L^2(K)}.$$

As proved in Ref. 22, $\left\|v^i(\cdot,t)\right\|_{L^2(K)}$ is absolutely continuous in time, and the result is obtained by Gronwall's inequality. □

Remark 4.1. *It is easy to prove that* $\lambda_0 \geq \frac{\alpha}{C_P^2}$*, where the Poincaré constant for a convex domain* K *is* $C_P = \frac{diam(K)}{\pi}$*, see Ref. 39. Here, we assume to know exactly* $diam(K)$*. In practice, it can often be estimated.*

Lemma 4.3 (Truncation error)**.** *Let* $v^i \in C([0,+\infty), L^2(K))$ *solve* (10)*, and let*

$$I_{ij}^4 := 2\int_T^{+\infty} \fint_K v^i(\mathbf{x},t)v^j(\mathbf{x},t)d\mathbf{x}\,dt.$$

Then, there exist $C_4 > 0$*, independent of* T*, such that*

$$\left|I_{ij}^4\right| \leq C_4 e^{-2\lambda_0 T}, \tag{23}$$

where λ_0 *is the smallest eigenvalue of* B*.*

Proof. We start by applying the Cauchy-Schwarz inequality on $L^2(K)$:

$$\left|I_{ij}^4\right| \leq \frac{2}{|K|}\int_T^{\infty} \left\|v^i(\cdot,t)\right\|_{L^2(K)} \left\|v^j(\cdot,t)\right\|_{L^2(K)} dt. \tag{24}$$

Then, we plug the result of Lemma 4.2 into (24):

$$\begin{aligned}\left|I_{ij}^4\right| &\leq \frac{2}{|K|}\int_T^{\infty} e^{-2\lambda_0 t} \left\|v^i(\cdot,0)\right\|_{L^2(K)} \left\|v^j(\cdot,0)\right\|_{L^2(K)} dt \\ &\leq \frac{1}{|K|} \left\|v^i(\cdot,0)\right\|_{L^2(K)} \left\|v^j(\cdot,0)\right\|_{L^2(K)} \frac{1}{\lambda_0} e^{-2\lambda_0 T}.\end{aligned}$$

The result follows by choosing

$$\begin{aligned}C_4 &= \frac{1}{\lambda_0 |K|} \left\|v^i(\cdot,0)\right\|_{L^2(K)} \left\|v^j(\cdot,0)\right\|_{L^2(K)} \\ &= \frac{1}{\lambda_0 |K|} \left\|\nabla\cdot(a(\cdot)\mathbf{e}_i)\right\|_{L^2(K)} \left\|\nabla\cdot(a(\cdot)\mathbf{e}_j)\right\|_{L^2(K)}.\end{aligned}$$

□

4.3 Bound for I_{ij}^2

From the definition,

$$I_{ij}^2 := 2\int_0^T \int_{K_L} \left(v^i v^j - u^i u^j\right) \mu_L \, d\mathbf{x}\, dt, \tag{25}$$

one can notice that the source of the error I_{ij}^2 is the mismatch between u^i and v^i on the boundary ∂K_R. Therefore, we refer to such an error as the *boundary* error. The boundary error converges to zero at an exponential rate, as stated in Lemma 4.4.

Lemma 4.4. *Let assumptions* (18) *be satisfied, let* I_{ij}^2 *be defined by* (25), $0 < L < R-2$, $T < \frac{2\nu}{d}\left|\tilde{R}-L\right|^2$ *and* $T < \tilde{C}_{2,c}\,|R-L|$, *where the constants* $\nu, \tilde{C}_{2,c} > 0$ *are defined in Theorem* 4.1 *and Proposition* 4.2, *respectively. Then, there exists a constant* $C > 0$ *and a constant* $0 < c \leq \nu$, *independent of* R, L *and* T *such that*

$$\left|I_{ij}^2\right| \leq C\left[\frac{R^{d-1}}{T^{d/2}}e^{-c\frac{|R-L|^2}{T}} + \frac{R^{2(d-1)}}{T^d}e^{-2c\frac{|R-L|^2}{T}}\right].$$

The proof of Lemma 4.4 directly follows from Propositions 4.1 and 4.2. We need Definitions 4.1 and 4.2 in order to define a *boundary error function* which will be used in the estimation of I_{ij}^2.

Definition 4.1 (Boundary layer)**.** *Let us define a sub-domain* $K_{\tilde{R}} \subset K_R$, *where* $\tilde{R}$ *is defined to be the largest integer such that* $\tilde{R} \leq R-1/2$. *The* boundary layer *is defined as the set* $\Delta := K_R \setminus K_{\tilde{R}}$. *We observe that* $|\Delta| = R^d - \tilde{R}^d \leq 2dR^{d-1}$.

Definition 4.2 (Cut-off function)**.** *A* cut-off function *on* K_R *is a function* $\rho \in C^\infty(K_R, [0,1])$ *such that*

$$\rho(\mathbf{x}) = \begin{cases} 1 \text{ in } K_{\tilde{R}} \\ 0 \text{ on } \partial K_R \end{cases} \qquad \text{and} \quad |\nabla\rho(\mathbf{x})| \leq C_\rho \text{ on } \Delta,$$

where the subdomain $K_{\tilde{R}}$ *and the boundary layer* Δ *are defined according to Definition* 4.1.

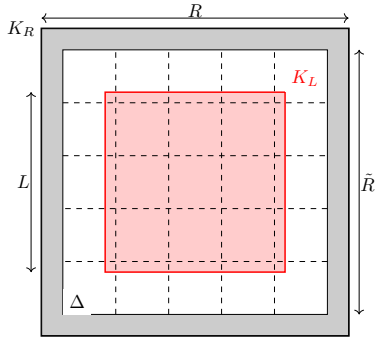


Figure 1: Scheme of the sampling domain K_R and its subsets K_L, $K_{\tilde{R}}$ and Δ.

Let us define the boundary error function $\theta^i \in L^2\left([0,+\infty), H_0^1(K_R)\right)$ through the relation $\theta^i := u^i - \rho v^i$. For the analysis it is fundamental that $\rho = 1$ in $K_{\tilde{R}}$ and that $L < \tilde{R}$. By the definition of θ^i, we write

$$I_{ij}^2 = 2\int_0^T \int_{K_L} \left[v^i v^j\left(1-\rho^2\right) - \rho\left(\theta^i v^j + v^i\theta^j\right) - \theta^i\theta^j\right]\mu_L\, d\mathbf{x}\, dt.$$

One readily notice that the first term in the integral vanishes on the integration domain, since $\rho^2(\mathbf{x}) = 1$ for all $\mathbf{x} \in K_{\tilde{R}} \supset K_L$. So, we have to study the integrals

$$I_{ij}^{2,b} := \int_0^T \int_{K_L} v^i \theta^j \mu_L \, d\mathbf{x} \, dt, \quad \text{and} \quad I_{ij}^{2,c} := \int_0^T \int_{K_L} \theta^i \theta^j \mu_L \, d\mathbf{x} \, dt. \tag{26}$$

As both integrals depend on the values that the functions θ^i take over the averaging domain K_L, we need to provide pointwise estimates for $\theta^i(\mathbf{x}, t)$ on $K_L \times [0, T]$. This is done in subsection 4.3.1 by the use of the fundamental solution of problem (9).

4.3.1 Estimates for θ^i

Here, we derive an upper bound for θ^i on $K_L \times [0, T]$. Let us define

$$F(\mathbf{x}, t) := -\nabla(1 - \rho(\mathbf{x})) \cdot a(\mathbf{x}) \nabla v^i - \nabla \cdot \left[a(\mathbf{x}) v^i \nabla(1 - \rho(\mathbf{x})) \right]. \tag{27}$$

By definition and linearity of the correctors problem, the function θ^i satisfies

$$\begin{cases} \dfrac{\partial \theta^i}{\partial t} - \nabla \cdot (a(\mathbf{x}) \nabla \theta^i) = F(\mathbf{x}, t) & \text{in } K_R \times (0, +\infty), \\ \theta^i = 0 & \text{on } \partial K_R \times (0, +\infty), \\ \theta^i(\mathbf{x}, 0) = v^i(\mathbf{x}, 0)(1 - \rho(\mathbf{x})) & \text{in } K_R. \end{cases} \tag{28}$$

The pointwise values of $\theta^i(\mathbf{x}, t)$ can be estimated by making use the weak fundamental solution $G(\cdot, \cdot; \mathbf{y}) : (\mathbf{x}, t) \mapsto \mathbb{R}$, defined as the solution of

$$\begin{cases} \partial_t G(\cdot, \cdot; \mathbf{y}) - \nabla \cdot (a(\mathbf{x}) \nabla G(\cdot, \cdot; \mathbf{y})) = 0 & \text{in } K_R \times (0, +\infty) \\ G(\cdot, \cdot; \mathbf{y}) = 0 & \text{on } \partial K_R \times (0, +\infty) \\ G(\cdot, 0; \mathbf{y}) = \delta_{\mathbf{y}} & \text{in } K_R, \end{cases} \tag{29}$$

where $\delta_{\mathbf{y}}$ is the Dirac delta centred at $\mathbf{y}$ and thanks to the results stated in Theorem 4.1.

Theorem 4.1 (Theorem 9 in Ref. 14)**.** *Assume $a(\cdot) \in \mathcal{M}(\alpha, \beta, K_R)$, $\theta^i(\cdot, 0) \in L^2(K_R)$ and $F \in L^q((0, T), L^p(K_R))$, with $1 < p, q \leq \infty$ and $\frac{d}{2p} + \frac{1}{q} \leq 1$. Then,*

a) $G(\mathbf{x}, t; \mathbf{y}) = G(\mathbf{y}, t; \mathbf{x})$ for $\mathbf{x} \in K_R$, $\mathbf{y} \in K_R$ and $t > 0$.

b) For each $\mathbf{y} \in K_R$, $G(\cdot, \cdot; \mathbf{y})$ is continuous in $K_R \times (0, T)$.

c) The Nash–Aronson estimate

$$0 \leq G(\mathbf{x}, t; \mathbf{y}) \leq \frac{C}{t^{d/2}} e^{-\nu \frac{|\mathbf{x} - \mathbf{y}|^2}{t}}, \tag{30}$$

holds true with $C(\alpha, \beta, d) > 0$ and $\nu(\beta, d) > 0$.

d) For fixed $\mathbf{y}$ and arbitrary $\tau \in (0, T)$, $G(\cdot, \cdot; \mathbf{y}) \in L^2((\tau, T), H_0^1(K_R))$.

e) For any $t > 0$, the weak solution θ^i of (28) can be represented by:

$$\theta^i(\mathbf{x},t) = \int_{K_R} G(\mathbf{x},t;\mathbf{y}) v^i(\mathbf{y},0)(1-\rho(\mathbf{y}))\,d\mathbf{y} + \int_{K_R}\int_0^t G(\mathbf{x},t-s;\mathbf{y}) F(\mathbf{y},s)\,ds\,d\mathbf{y}. \quad (31)$$

Remark 4.2. *The practical choice of parameters in the numerical simulations requires to estimate the constant ν of (30). According to Ref. 14 (equation (7.12)), ν can be estimated as $\nu = \gamma/8$, where γ (which is called α in Ref. 14, Lemma 1) depends only on the dimension d and the constant β in Definition 2.2.*

A straightforward computation using the definition of F, (27), shows that assumptions (18b) and (18c) in Theorem 3.2 are needed in order to ensure that $F \in L^q((0,T), L^p(K_R))$, with $1 < p, q \leq \infty$ and $\frac{d}{2p} + \frac{1}{q} \leq 1$. In the proofs of our main theorem we will use the following reformulation of θ^i, using the definition of F and integration by parts:

$$\begin{aligned}\theta^i(\mathbf{x},t) = &\int_{K_R} G(\mathbf{x},t;\mathbf{y}) v^i(\mathbf{y},0)(1-\rho(\mathbf{y}))\,d\mathbf{y} \\ &- \int_{K_R}\int_0^t G(\mathbf{x},t-s;\mathbf{y}) \nabla_{\mathbf{y}}(1-\rho(\mathbf{y})) \cdot a(\mathbf{y}) \nabla_{\mathbf{y}} v^i(\mathbf{y},s)\,ds\,d\mathbf{y} \\ &+ \int_{K_R}\int_0^t \nabla_{\mathbf{y}} G(\mathbf{x},t-s;\mathbf{y}) \cdot a(\mathbf{y}) \nabla_{\mathbf{y}}(1-\rho(\mathbf{y})) v^i(\mathbf{y},s)\,ds\,d\mathbf{y}. \quad (32)\end{aligned}$$

An upper bound estimate for $\theta^i(\mathbf{x},t)$ on K_L is given in the following lemma, whose proof is postponed to A.

Lemma 4.5. *Let assumptions (18) be satisfied, $0 < L < R-2$ and θ^i be the solution of (28). Then, there exist constants $C_1, C_2 > 0$ and $0 < c \leq \nu$ (where ν is the constant in (30)), independent of R and L, such that, for any $0 < t < 2\nu \left|\tilde{R} - L\right|^2$,*

$$\left\|\theta^i(\cdot,t)\right\|_{L^\infty(K_L)} \leq C_1 \left\|\nabla \cdot (a(\cdot)\mathbf{e}_i)\right\|_{L^2(K)} \left(1 + C_2 \frac{t}{|R-L|}\right) \frac{R^{d-1}}{t^{d/2}} e^{-c\frac{|R-L|^2}{t}}. \quad (33)$$

4.3.2 Term $I^{2,b}$

Proposition 4.1. *Let the hypotheses of Lemma 4.5 be satisfied. Moreover, let $I_{ij}^{2,b}$ be defined as in (26), $R \geq 1$ and $T < \frac{2\nu}{d}\left|\tilde{R} - L\right|^2$. Then, there exist constants $C_{2,b} > 0$ and $0 < c \leq \nu$ independent of R, L, T such that*

$$\left|I_{ij}^{2,b}\right| \leq C_{2,b} \frac{R^{d-1}}{T^{d/2}} e^{-c\frac{|R-L|^2}{T}}. \quad (34)$$

Proof. Applying Hölder inequality on the space integral, we obtain:

$$I_{ij}^{2,b} \leq \int_0^T \left\|v^i(\cdot,t)\right\|_{L^2(K_L)} \left\|\theta^j(\cdot,t)\right\|_{L^\infty(K_L)} \|\mu_L\|_{L^2(K_L)}\, dt.$$

By assumption, $\mu_L \in L^\infty(K_L) \subset L^2(K_L)$ with continuous inclusion, and by the definition of the filter (see Section 2), we have

$$\|\mu_L\|_{L^2(K_L)} \leq |K_L|^{1/2} \|\mu_L\|_{L^\infty(K_L)} \leq C_\mu L^{-d/2}.$$

Next, we estimate $\left\|v^i(\cdot,t)\right\|_{L^2(K_L)}$. Since v^i is K-periodic we have, for integer L,

$$\left\|v^i(\cdot,t)\right\|_{L^2(K_L)} = L^{d/2} \left\|v^i(\cdot,t)\right\|_{L^2(K)},$$

while, for non-integer L

$$\left\|v^i(\cdot,t)\right\|_{L^2(K_L)} \leq \lceil L \rceil^{d/2} \left\|v^i(\cdot,t)\right\|_{L^2(K)}.$$

Finally, we recall the exponential decay of $\left\|v^i(\cdot,t)\right\|_{L^2(K)}$ and we derive the estimate:

$$\begin{aligned} I_{ij}^{2,b} &\leq L^{d/2} \|\nabla \cdot (a(\cdot)\mathbf{e}_i)\|_{L^2(K)} \int_0^T e^{-\lambda_0 t} \left\|\theta^j(\cdot,t)\right\|_{L^\infty(K_L)} dt\, C_\mu L^{-d/2} \\ &\leq C_\mu \|\nabla \cdot (a(\cdot)\mathbf{e}_i)\|_{L^2(K)} \int_0^T e^{-\lambda_0 t} \left\|\theta^j(\cdot,t)\right\|_{L^\infty(K_L)} dt. \quad (35) \end{aligned}$$

Since $T < \frac{2\nu}{d}\left|\tilde{R} - L\right|^2$, the assumption on t of Lemma 4.5 are satisfied and we can use (33) to bound the last integral in (35):

$$\begin{aligned} &\int_0^T e^{-\lambda_0 t} \left\|\theta^j(\cdot,t)\right\|_{L^\infty(K_L)} dt \leq \\ &\leq C_1 \|\nabla \cdot (a(\cdot)\mathbf{e}_i)\|_{L^2(K)} R^{d-1} \int_0^T \left(1 + C_2 \frac{t}{|R-L|}\right) e^{-\lambda_0 t} t^{-d/2} e^{-c\frac{|R-L|^2}{t}} dt \\ &\leq C_1 \|\nabla \cdot (a(\cdot)\mathbf{e}_i)\|_{L^2(K)} R^{d-1} \max_{t\in[0,T]} \left(t^{-d/2} e^{-c\frac{|R-L|^2}{t}}\right) \int_0^T \left(1 + C_2 \frac{t}{|R-L|}\right) e^{-\lambda_0 t} dt \\ &= \frac{C_1}{\lambda_0} \|\nabla \cdot (a(\cdot)\mathbf{e}_i)\|_{L^2(K)} R^{d-1} \left(1 + \frac{C_2}{\lambda_0 |R-L|}\right) \max_{t\in[0,T]} \left(t^{-d/2} e^{-c\frac{|R-L|^2}{t}}\right). \end{aligned}$$

From the fact that $t^{-d/2} e^{-c\frac{|R-L|^2}{t}}$ is strictly increasing in $(0,T)$, with $T < \frac{2\nu}{d}\left|\tilde{R} - L\right|^2$, we have

$$\max_{t\in[0,T]} \left(t^{-d/2} e^{-c\frac{|R-L|^2}{t}}\right) = T^{-d/2} e^{-c\frac{|R-L|^2}{T}}.$$

Then, we get (34) by posing

$$C_{2,b} = \frac{C_\mu C_1}{\lambda_0}\left(1+\frac{C_2}{\lambda_0\left|R-L\right|}\right)\left\|\nabla\cdot(a(\cdot)\mathbf{e}_i)\right\|^2_{L^2(K)}$$
$$\leq \frac{C_\mu C_1}{\lambda_0}\left(1+\frac{C_2}{\lambda_0(1-k_o)}\right)\left\|\nabla\cdot(a(\cdot)\mathbf{e}_i)\right\|^2_{L^2(K)},$$

since $R \geq 1$. □

4.3.3 Term $I^{2,c}$

Here, we provide estimates for the term $I^{2,c}_{ij}$ of (26). This term decays faster than $I^{2,b}_{ij}$ and can be considered negligible.

Proposition 4.2. *Let the hypotheses of Lemma* 4.5 *be satisfied. Moreover, let* $I^{2,c}_{ij}$ *be defined as in* (26) *and* $T < \frac{2\nu}{d}\left|\tilde{R}-L\right|^2$. *If* $\tilde{C}_{2,c} > 0$ *is a constant independent of* T, R *and* L, *such that* $T < \tilde{C}_{2,c}(R-L)$, *then there exist constants* $C_{2,c} > 0$ *and* $0 < c \leq \nu$ *independent of* R, L, T *such that*

$$\left|I^{2,c}_{ij}\right| \leq C_{2,c}\frac{R^{2(d-1)}}{T^d}e^{-2c\frac{|R-L|^2}{T}}. \tag{36}$$

Proof. From the positivity of μ_L and the fact that it has unit mass, we derive the inequality

$$\left|\int_0^T\int_{K_L}\theta^i(\mathbf{x},t)\theta^j(\mathbf{x},t)\mu_L(\mathbf{x})\,d\mathbf{x}\,dt\right| \leq \max_i\int_0^T\left\|\theta^i(\cdot,t)\right\|^2_{L^\infty(K_L)}\,dt.$$

From Lemma 4.5 the term on the right-hand side can be estimated by:

$$\int_0^T\left\|\theta^i(\cdot,t)\right\|^2_{L^\infty(K_L)}\,dt \leq$$
$$\leq C_1^2\left\|\nabla\cdot(a(\cdot)\mathbf{e}_i)\right\|^2_{L^2(K)}\int_0^T\left(1+C_2\frac{t}{|R-L|}\right)^2\frac{R^{2(d-1)}}{t^d}e^{-2c\frac{|R-L|^2}{t}}\,dt$$
$$\leq \frac{C_1^2}{2c}\left\|\nabla\cdot(a(\cdot)\mathbf{e}_i)\right\|^2_{L^2(K)}\left(1+C_2\frac{T}{|R-L|}\right)^2\frac{T^2}{|R-L|^2}\frac{R^{2(d-1)}}{T^d}e^{-2c\frac{|R-L|^2}{T}},$$

hence (36) follows by defining

$$C_{2,c} := \frac{C_1^2}{2c}\left\|\nabla\cdot(a(\cdot)\mathbf{e}_i)\right\|^2_{L^2(K)}\left(1+C_2\frac{T}{|R-L|}\right)^2\frac{T^2}{|R-L|^2}$$
$$\leq \frac{C_1^2}{2c}\left\|\nabla\cdot(a(\cdot)\mathbf{e}_i)\right\|^2_{L^2(K)}\left(1+C_2\tilde{C}_{2,c}\right)^2\tilde{C}^2_{2,c}.$$

□

Now, we are ready to prove Theorem 3.2.

Theorem 3.2. The decomposition (21) implies

$$\left\|a^0_{R,L,T} - a^0\right\|_F \leq d^2 \max_{i,j} \left(\left|I^1_{ij}\right| + \left|I^2_{ij}\right| + \left|I^3_{ij}\right| + \left|I^4_{ij}\right|\right).$$

By using the upper bounds in Corollary 4.1, Lemmas 4.1 and 4.3, and Propositions 4.1 and 4.2 in the above inequality we get

$$\left\|a^0_{R,L,T} - a^0\right\|_F \leq C\left[L^{-(q+1)} + e^{-2\lambda_0 T} + \frac{R^{d-1}}{T^{d/2}} e^{-c\frac{|R-L|^2}{T}} + \frac{R^{2(d-1)}}{T^d} e^{-2c\frac{|R-L|^2}{T}}\right], \tag{37}$$

for some constant C independent of R, L and T. Using the optimal values $L = k_o R$ and $T = k_T(R-L)$, with $0 < k_o < 1$ and $k_T = \sqrt{\frac{c}{2\lambda_0}}$, we write (37) as:

$$\left\|a^0_{R,L,T} - a^0\right\|_F \leq C\Bigg[R^{-(q+1)} + e^{-\sqrt{2\lambda_0 c}(1-k_o)R} + R^{d/2-1} e^{-\sqrt{2\lambda_0 c}(1-k_o)R} + R^{d-2} e^{-2\sqrt{2\lambda_0 c}(1-k_o)R}\Bigg]$$

The last term is of higher order than the third one, so it can be omitted. Finally, we get

$$\left\|a^0_{R,L,T} - a^0\right\|_F \leq C\left[R^{-(q+1)} + \left(1 + R^{d/2-1}\right) e^{-\sqrt{2\lambda_0 c}(1-k_o)R}\right]. \tag{38}$$

□

5 Numerical tests

In this section we present several numerical tests which support the theoretical results of Section 4 and experimentally verify the resonance error bound of Theorem 3.2. We illustrate the expected convergence rates by varying the regularity parameter q of the filters, in a periodic, smooth setting, as rigorously proven in the previous sections. Additionally, we compare the convergence rate of the resonance error for the parabolic scheme with that of the regularised elliptic method described in Ref. 24. We also test non-smooth periodic and non-periodic coefficients (a realization of a log-normal field) to test our algorithm beyond the periodic setting and for which we obtain good results as in the smooth periodic case.

In order to numerically assess the convergence rate of the resonance error, we compute the approximations of the homogenized tensor through the described parabolic cell problems on domains of increasing size, $R \in [1, 20]$, and calculate the resonance error as the Frobenius norm of the difference between the

numerical approximation of $a^0_{R,L,T}$ (here still denoted as $a^0_{R,L,T}$) and the exact a^0:

$$err = \left\| a^0_{R,L,T} - a^0 \right\|_F . \tag{39}$$

In the case of periodic coefficients whose homogenized value could not be known exactly (i.e., without discretization error) the reference value is computed by solving the standard elliptic micro problem (5)and periodic boundary conditions and using formula (4). In the random setting no approximation is available without some resonance error. In this case, we take as reference value for the homogenized tensor the one computed from the numerical approximation of the parabolic correctors over the largest domain $R_{max} = 20$.

To compute a numerical approximation of $a^0_{R,L,T}$, we use a Finite Elements (FE) discretization for the micro problems (9) in space, and a stabilised explicit Runge-Kutta method with adaptive time stepping for the time discretization. The fourth order explicit stabilised method ROCK4 , Ref. 1, with fine tolerance is chosen when we want to kill the discretization error in time, while the second order explicit stabilised method ROCK2, Ref. 7, with tolerances adapted to the spatial discretization error is chosen when we test the efficiency of the parabolic approach. As we use explicit methods in time, we need a mass matrix that is cheap to invert. This is achieve by using either mass lumping (for low order FEMs) or discontinuous Galerkin methods (for arbitrary order FEMs).

As a second step, the upscaled tensor is approximated by a double integration in space and time. The spatial integral of the parabolic correctors is computed by using the FE filtered mass matrix of components

$$m_{ij} = \int_{K_L} \phi_i(\mathbf{x})\phi_j(\mathbf{x})\mu_L(\mathbf{x})\, d\mathbf{x},$$

where $\{\phi_i\}_i$ are the FE basis functions. The integration in time is performed by the use of a Newton-Cotes formula for non-uniform discretizations, in particular the Simpson's rule.

In order to optimize the convergence rate of the error with respect to the sampling domain size R, we take the optimal values for the averaging domain size L ($K_L \subset K_R$) and for the final time T given by

$$L = k_o R, \text{ and } \quad T = \sqrt{\frac{1}{4\pi^2\alpha\beta}}\, |R - L| , \tag{40}$$

where α and β are the ellipticity and continuity constants of the tensor a. This choice for T comes from the optimal value given in Theorem 3.2, with the lower bound for $\lambda_0 \geq \frac{\alpha\pi^2}{diam(K)^2}$ (see Remark 4.1). For the practical estimation of the constant c we use $c = (4\beta)^{-1}$ (this value is derived in Ref. 13, Chapter 8, Section 5 for unbounded domains). Note that β is computed as $\beta = \|a\|_{L^\infty(\mathbb{R}^d)}$. The value of $diam(K) = \sqrt{2}$ is used to derive (40), as we assigned the periodic cell to be $(-1/2, 1/2)^2$. In practical situations where $diam(K)$ is not known exactly, it can often be roughly estimated. The oversampling ratio, $0 < k_o < 1$, and the order of filters, q, can be chosen freely.

5.1 Two-dimensional periodic case

We consider the upscaling of the 2×2 isotropic tensor:

$$a(\mathbf{x}) = \left(\frac{2 + 1.8 \sin(2\pi x_1)}{2 + 1.8 \cos(2\pi x_2)} + \frac{2 + \sin(2\pi x_2)}{2 + 1.8 \cos(2\pi x_1)} \right) \mathrm{Id} \tag{41}$$

for which the homogenized tensor is

$$a^0 \approx \begin{pmatrix} 2.757 & -0.002 \\ -0.002 & 3.425 \end{pmatrix}.$$

Here, we compare the performances of the described parabolic approach ("par." in the legends), the standard elliptic approach ("ell." in the legends) and the regularised elliptic approach of Ref. 24. In comparing the different methods, we used a filtered version of (6), namely

$$\mathbf{e}_i \cdot a^0_{R,L} \mathbf{e}_j := \int_{K_L} \mathbf{e}_i \cdot a(\mathbf{x}) \left(\mathbf{e}_j + \nabla \chi^j_R(\mathbf{x}) \right) \mu_L(\mathbf{x}) \, d\mathbf{x}, \tag{42}$$

that improves the error constant for the classical approach. However, we recall that the standard elliptic method provides a first order convergence rate, independently of the use of oversampling or filtering, as shown in Ref. 43. By contrast, the use of high order filters in the parabolic and regularised elliptic schemes improves the convergence rate without affecting the computational cost.

All the approaches are solved using $\mathbb{P}1$ finite element discretization in space with 64 points per periodic cell. Mass lumping has been used in order to perform the time integration, which is carried out via the fourth order explicit stabilised ROCK4 method, see Ref. 1, with $tol = 10^{-6}$ (since we want to kill the discretization error in time). Finally Simpson's quadrature rule is used for computing the time integral defining homogenized coefficients.

Results are depicted in Figure 2. As expected, one cannot reach a convergence rate higher than 1 for the standard elliptic approach, in contrast to the regularised elliptic and parabolic methods. For low order filters ($q = 1$), we observe that both the parabolic approach and the regularised elliptic approach have the same convergence rate but the latter has a smaller prefactor. As the parameter q gets larger, the parabolic approach starts to result in smaller resonance errors asymptotically (as R increases). The advantage of the parabolic approach over the regularised counterpart is more pronounced for larger values of q. This is also discussed in Section 6, where we investigate the computational efficiency. For all the three methods, we notice a longer "flat" region in the convergence plot for small values of k_o and high order filters. Intuitively, for any given R, the region where the filter is "not almost zero" decreases for smaller k_o and larger q. Hence, we need larger values of R for the averaging integral to contain enough data and the error to decrease with the expected rate.

We conclude this section by showing the effect that different values of k_T have on the convergence rate. In Figure 3, the resonance error is plotted against

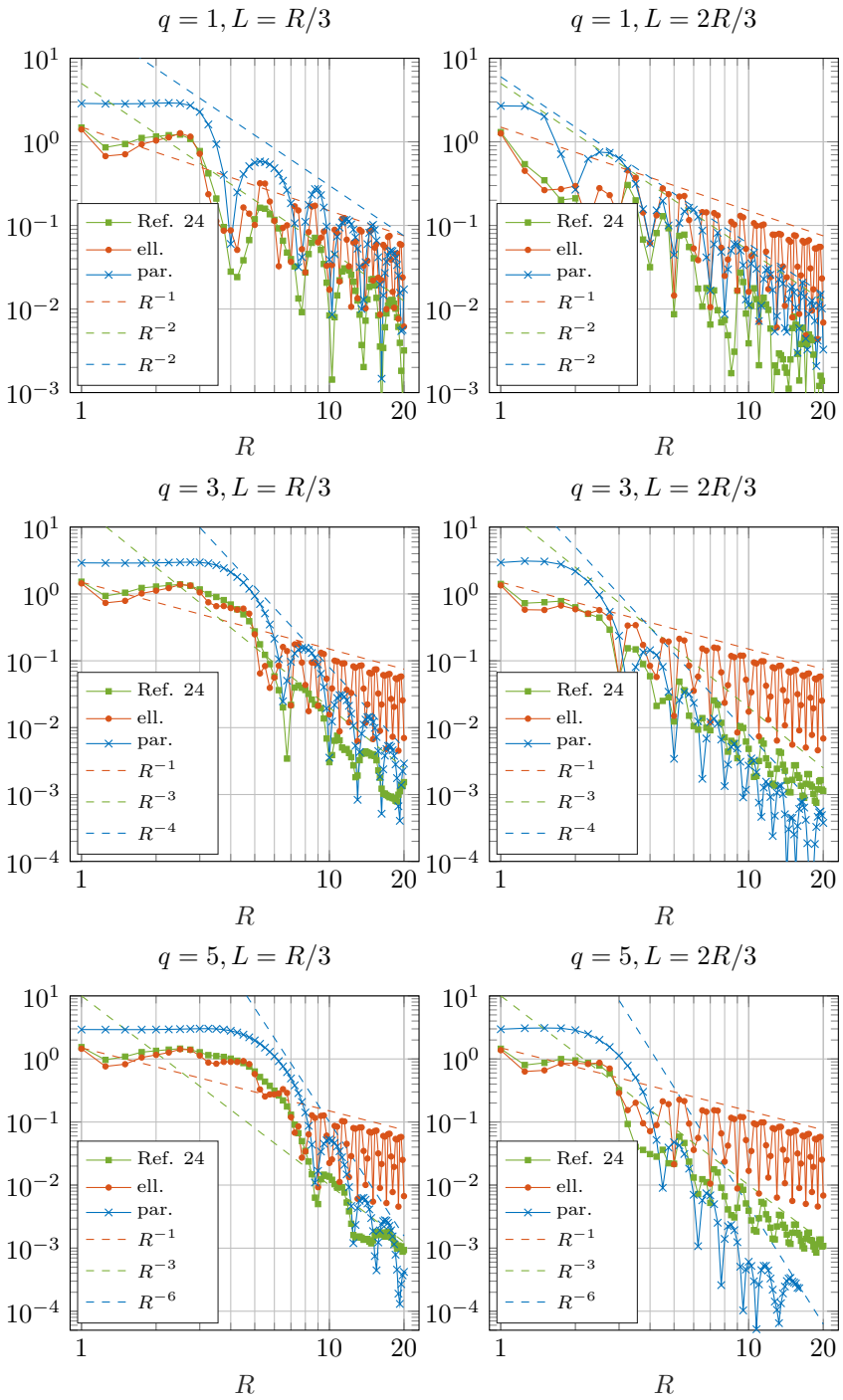


Figure 2: Comparison of the resonance error in the standard elliptic, regularised elliptic and parabolic models for the tensor (41). The size of the sampling domain, R, is reported on the x-axis; the resonance error (39) is reported on the y-axis.

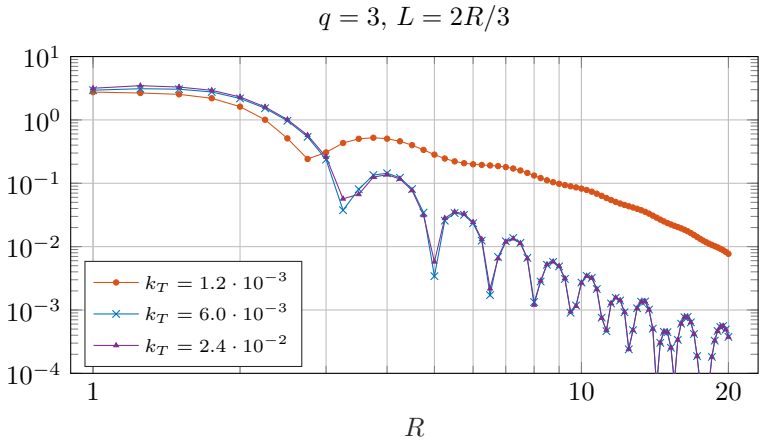


Figure 3: Effect of using different values of k_T. The size of the sampling domain, R, is reported on the x-axis; the resonance error (39) is reported on the y-axis.

the value of R, for the choice of $k_o = 2/3$, $q = 3$, and three different values for k_T. The results clearly show that if k_T is much smaller than the optimal value then the error convergence is severely hampered (see the first plot in Figure 3), so the error is dominated by the truncation error ($e^{-2\lambda_0 T}$ in Theorem 3.2). However, note that, as R gets larger the exponentially decaying errors will be dominated by the averaging error and the asymptotic decay rate of Theorem 3.2 will be recovered. On the other hand, the results do not vary sensibly if larger values for k_T are used, even though they are not the "optimal" ones, see the plots for $k_T = 6.0 \cdot 10^{-3}$ and $k_T = 2.4 \cdot 10^{-2}$. In those cases the main contribution to the resonance error comes from the averaging error terms, which do not depend on k_T. The fact that the same convergence behaviour is achieved for a large range of k_T values allows to choose it with a high degree of flexibility.

5.2 Non-smooth coefficients

In the example above, we have considered smooth coefficients. We will now present the results for an example with the non-smooth periodic coefficients:

$$a(x) = \begin{cases} 1 & x \in \mathbb{Z} + K_{1/4}, \\ 12\,\|x - [x]\|_\infty - \frac{1}{2} & x \in \mathbb{Z} + (K_{3/4} \setminus K_{1/4}), \\ 4 & \text{elsewhere}, \end{cases} \tag{43}$$

where the components of $[x]$ are the integer values closest to x, component-wise. The diffusion coefficient field is depicted in Figure 4. The field (43) could be considered as an approximation of a composite material made up of low-diffusive square inclusions into an homogeneous medium. The case of discontinuous coefficients can still be tackled numerically, but an appropriate discontinuous

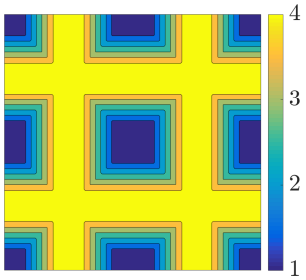


Figure 4: Visualization of the diffusion coefficient field (43)

Galerkin method needs to be implemented to get high orders in spatial discretization and thereby observe the asymptotic rate of the convergence. Convergence plots pictured in Figure 5 demonstrates that the theoretical results also apply to the case of non-smooth coefficients. The test is done with $\mathbb{P}1$ finite element discretization on a uniform grid of size $h = 1/128$ and the ROCK4 time integration scheme with $tol = 10^{-6}$. The final time T has been chosen according to (40). The results agree with both the previous example and the theoretical convergence rates. As before, the effect of having a smaller ratio $L/R = k_o$ is the increase in the length of the initial "flat" region, indicating that larger values of k_o are preferable. The resonance error converges as R^{-q-1}, where q is the order of the filters, independently from other parameters. Both the results for the regularised elliptic and parabolic methods are presented: the errors for both methods are comparable for $k_o = 2/3$ and $q = 2$, while the parabolic scheme shows faster decay of the error when $q = 4, 5$.

5.3 A non-periodic case

In the last numerical test, we provide an example for a non-periodic tensor which violates the periodicity assumption made in Section 4. With this test, we do not aim at proving any theoretical convergence rate of the error, but rather to verify numerically that the periodicity assumption is not necessary for achieving fast decaying rates of the boundary error. We consider a single realization of a stationary log-normal random field with Gaussian isotropic covariance:

$$\log a(\cdot) \sim \mathcal{N}(\mu, Cov(\mathbf{x} - \mathbf{y})), \quad Cov(\mathbf{z}) = \sigma^2 e^{-\frac{|\mathbf{z}|^2}{2\ell^2}}, \tag{44}$$

where μ and σ^2 are the mean and the variance of the field and ℓ is the correlation length. An example of such a field is depicted in Figure 6a. Here, the choice of $\ell = 0.2$ has been made, in order to include enough oscillations in the unit cell $[-1/2, 1/2]^2$ We are not interested in evaluating the statistical error, but only

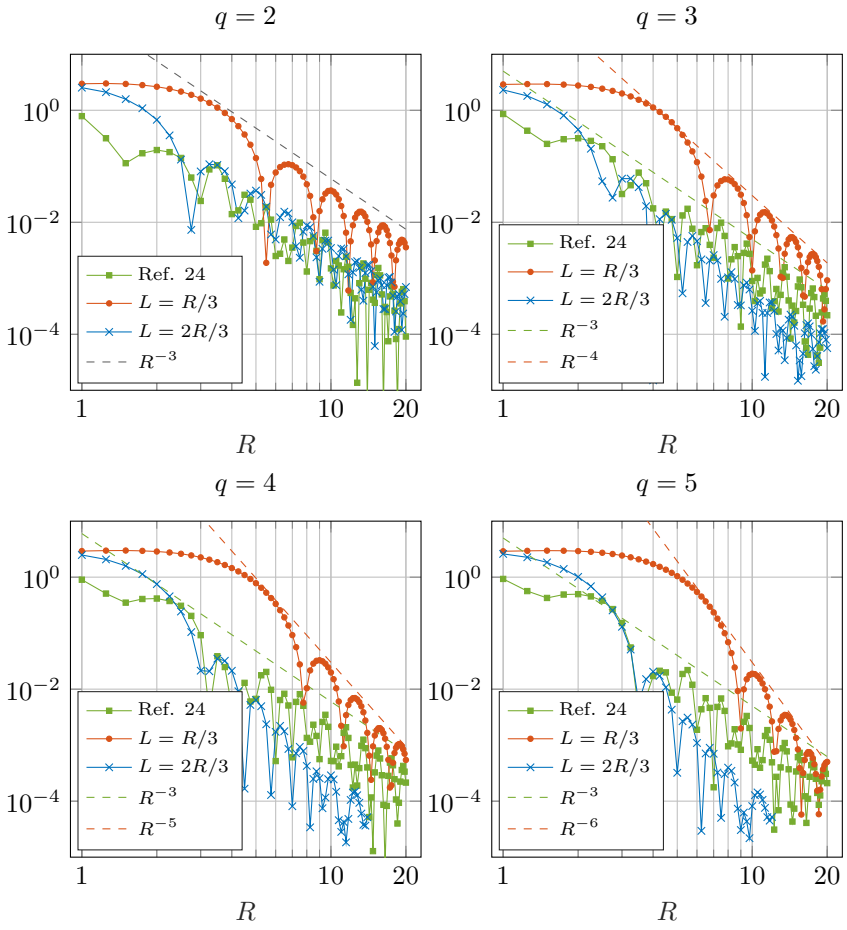
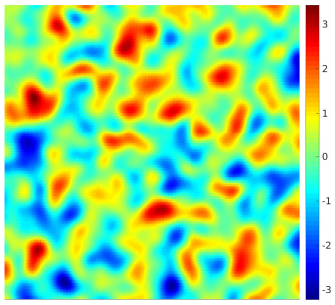


Figure 5: Comparison of the resonance error in the regularised elliptic and parabolic models for the non-smooth tensor (43). The size of the sampling domain, R, is reported on the x-axis; the resonance error (39) is reported on the y-axis.

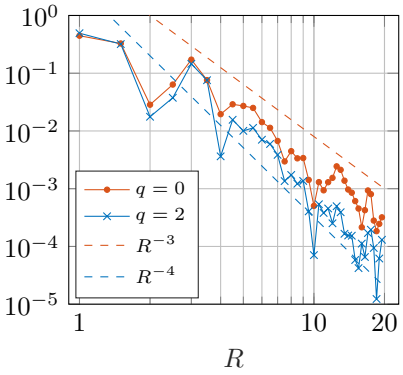
the boundary error, which is

$$\left\| a^0_{R,L,T} - a^0_{\infty,L,T} \right\|_F .$$

In practice, we will consider $a^0_{R_{max},L,T}$ for the large value $R_{max} = 20$ in place of $a^0_{\infty,L,T}$ as a reference for evaluating the resonance error. The new reference $a^0_{R_{max},L,T}$ is computed using the numerical approximation of the parabolic corrector on $K_{R_{max}}$ with periodic BCs. The test is done with a $\mathbb{P}1$ finite element discretization on a uniform grid of size $h = 1/20$ and the ROCK4 time integration scheme with $tol = 10^{-5}$. In Figure 6b we show that the resonance error decays with a rate comprised between 3 and 4 with respect to R.



(a) Realization of the field on the square $[-2,2]^2$. The colour scale is logarithmic.



(b) Resonance error. $L = 2R/3$.

Figure 6: Log-normal random field (44) with $\mu = 0$, $\sigma^2 = 1$ and $\ell = 0.2$, and resonance error for the parabolic cell problem with filter order q and final time $T = \frac{|R-L|}{10}$. The size of the sampling domain, R, is reported on the x-axis; the resonance error (39) is reported on the y-axis.

6 Computational efficiency

The goal of this section is to study the computational efficiency of the parabolic method. We will also provide theoretical and computational efficiency comparisons with the classical and the regularised elliptic methods. Our analysis and numerical computations show that, for sufficiently high order filters, the computational cost is lower for the parabolic model than for the elliptic ones.

6.1 Regularised elliptic model

Let us consider the regularised elliptic homogenization scheme described in Ref. 24, which reads as

$$\frac{1}{T}\psi^i_{R,T} - \nabla\cdot\big(a(\mathbf{x})\nabla\psi^i_{R,T}(\mathbf{x})\big) = \nabla\cdot a(\mathbf{x})\mathbf{e}_i, \quad \text{in } K_R \tag{45}$$

equipped with homogeneous Dirichlet BCs on ∂K_R. We partition the domain K_R with uniform simplicial elements of size h and we introduce a finite elements space $S_h \subset H^1_0(K_R)$ made of piecewise polynomial functions of degree s on the simplices. The finite elements discretization of the corrector problem reads: Find $\psi^i_{R,T,h} \in S_h$ such that

$$\int_{K_R} \frac{1}{T}\psi^i_{R,T,h}w_h + a(\mathbf{x})\left(\nabla\psi^i_{R,T,h} + \mathbf{e}_i\right)\cdot\nabla w_h\, d\mathbf{x} = 0, \quad \forall w_h \in S_h, \quad i = 1,\dots,d, \tag{46}$$

and the upscaled tensor is defined as (we only indicate the R parameter, as the optimal values L and T depend on R)

$$a_{ij}^{0,R,h} = \int_{K_L} \left(\nabla \psi_{R,T,h}^i + \mathbf{e}_i\right) \cdot a(\mathbf{x}) \left(\nabla \psi_{R,T,h}^j + \mathbf{e}_j\right) \mu_L(\mathbf{x})\, d\mathbf{x}. \tag{47}$$

Hence, the total error for the upscaled coefficients is:

$$|a_{ij}^{0,R,h} - a_{ij}^0| \lesssim h^{s+1} + R^{-4}(\log R)^8,$$

where the second term in the error estimate is the modelling error. The finite elements corrector $\psi_{R,h}^i$ is computed by solving the linear system

$$A_h \mathbf{v}_i = \mathbf{b}_i, \text{ for } i = 1, \ldots, d, \tag{48}$$

where A_h is a $N \times N$ symmetric positive definite matrix and $\mathbf{v}_i$ and $\mathbf{b}_i$ are the coordinates of, respectively, ψ_h and $-\nabla \cdot (a(y)\mathbf{e}_i)$ in the finite element space and given a lagrangian basis. Here, $N = \mathcal{O}(R^d h^{-d})$ is the dimension of the space S_h. The linear system can be solved in several ways using direct or iterative methods, whose cost depends on N. For example, for LU factorization the number of operations is $\mathcal{O}(N^{3/2})$ Ref. 23, for Conjugate Gradient (CG) it is $\mathcal{O}(\sqrt{\kappa}N)$[4] Ref. 40, while for multigrid (MG) it is $\mathcal{O}(N)$. In the following analysis we will consider the LU factorization as linear solver, as it is the one that we used in practice to solve (46). We require the total errors to scale as a given tolerance tol, so $R = \mathcal{O}(tol^{-1/4})$ (we omitted the logarithmic term) and $h = \mathcal{O}(tol^{1/(s+1)})$. Hence, the total cost is

$$C = \mathcal{O}(N^{3/2}) = \mathcal{O}(R^{3d/2} h^{-3d/2}) = \mathcal{O}(tol^{-\frac{3d}{8} - \frac{3d}{2(s+1)}}).$$

6.2 Parabolic case with explicit stabilised time integration methods

Let us consider the parabolic cell problem (9) with the upscaling formula (13). As in the elliptic case, one can discretize (9) in space and compute an approximation $u_h^i(t)$ of $u^i(\cdot, t)$ in the N-dimensional finite elements space S_h. For simplicity of notation, we will omit the superscript i. For a given basis of S_h, the function $u_h(t)$ is uniquely determined by the vectorial function $\mathbf{w}_h : [0, T] \mapsto \mathbb{R}^N$, that solve the semi-discrete problem:

$$\frac{d}{dt}\mathbf{w}_h = -M_h^{-1} A_h \mathbf{w}_h. \tag{49}$$

We assume that the mass matrix M_h is easy to invert (which hold, e.g., in the case of mass lumping or discontinuous Galerkin FEs), so that the cost of the right-hand side evaluation is negligible with respect to the solution of the ODE

[4] κ is the condition number

system. The differential equation (49) is solved by an explicit stabilised time integration scheme of order r. Examples of second order methods are RKC2 (Ref. 42) and ROCK2 (Ref. 7), while ROCK4 (Ref. 1) is a fourth order method. The fully discrete problem reads

$$\mathbf{W}_k = \Phi_h(\mathbf{W}_{k-1}), \text{ for } k = 1, \dots, N_t,$$

where the function Φ_h identifies the time integration method and N_t the number of time steps. The computed sequence $\{\mathbf{W}_k\}_{k=0}^{N_t} \subset \mathbb{R}^N$ is an approximation, at times $t_k = k\Delta t$, of $\mathbf{w}(t_k)$ and it determines (via the finite elements basis) a sequence $\{U_k\}_{k=0}^{N_t} \subset S_h$. The discrete approximation of the homogenized tensor is

$$a_{ij}^{0,R,h,\Delta t} = \int_{K_L} a_{ij}(y)\mu_L(\mathbf{x})\, d\mathbf{x} - 2\mathcal{Q}\left(\int_{K_L} U_k U_k^j \mu_L(y)\, d\mathbf{x}, \Delta t\right),$$

where $\mathcal{Q}(\cdot, \Delta t)$ is a quadrature rule on the discretization $t_k = k\Delta t$ of order at least r (where r is the order of the time integration scheme). Hence, the total error for the upscaled coefficients is:

$$|a_{ij}^{0,R,h,\Delta t} - a_{ij}^0| \leq C\left(h^{s+1} + \Delta t^r + R^{-(q+1)}\right), \tag{50}$$

where we have assumed that, for sufficiently large R, the term $R^{-(q+1)}$ dominates the exponential term in the resonance error bound. This is also the convergence rate that we reported in the numerical examples of Subsections 5.1 and 5.2. Here, the constant C grows linearly with the final time T, whose optimal value scales as $R - L$. However, the ratio $(R-L)/\sqrt{8\beta\lambda_0}$ is in general $\mathcal{O}(1)$, so we can consider $T = \mathcal{O}(1)$ in the range of values used for R and L. In order for the error to scale as tol, we require that all the three summands in (50) scale as tol:

$$R = \mathcal{O}(tol^{-\frac{1}{q+1}}), \quad h = \mathcal{O}(tol^{\frac{1}{s+1}}), \quad \Delta t = \mathcal{O}(tol^{\frac{1}{r}}).$$

The global computational cost is $\mathcal{O}(N n_S N_t)$, where $N_t = T/\Delta t$ is the number of time steps, n_S is the number of function evaluations (stages) per time step for a stabilised method and $N = \mathcal{O}(R^d h^{-d})$ is the cost of each function evaluation which, in the linear case, is the cost of multiplying a sparse $N \times N$ matrix by a vector in $\mathbb{R}^N$. Since we are using a stabilised method we need to satisfy the weak stability condition $\rho\Delta t = c n_S^2$, where ρ is the spectral radius of the Jacobian of the ODE (49) and n_S is the number of stages for each time step. As ρ is the spectral radius of $M_h^{-1}A_h$, it scales as h^{-2}. Therefore, $n_S = \mathcal{O}(\Delta t^{1/2} h^{-1})$. From the fact that $T = \mathcal{O}(1)$ one derives that the total cost is

$$Cost = \mathcal{O}(R^d h^{-d} \Delta t^{1/2} h^{-1} \Delta t^{-1}) = \mathcal{O}(tol^{-\frac{d}{q+1} - \frac{d+1}{s+1} - \frac{1}{2r}}).$$

6.3 Comparison of the parabolic and the regularised elliptic models

We conclude the paper by comparing the computational cost of the elliptic regularised and the parabolic models. In Table 1, we summarize the dependency

of computational cost and the error on resonance and discretization parameters, as well as the scaling of the cost for a given tolerance.

Cell problem	Parabolic	Regularised Elliptic, Ref. 24
Error	$R^{-q-1} + h^{s+1} + \Delta t^r$	$R^{-4}(\log R)^8 + h^{s+1}$
Computational cost	$R^d h^{-d-1} \Delta t^{-\frac{1}{2}}$	$R^{3d/2} h^{-3d/2}$
Computational cost (tol)	$tol^{-\frac{d}{q+1} - \frac{d+1}{s+1} - \frac{1}{2r}}$	$tol^{-\frac{3d}{8} - \frac{3d}{2(s+1)}}$

Table 1: Error and computational cost for two homogenization approaches.

The parabolic approach will be asymptotically more efficient than the regularised elliptic one if:

$$\frac{d}{q+1} + \frac{d+1}{s+1} + \frac{1}{2r} < \frac{3d}{8} + \frac{3d}{2(s+1)}. \tag{51}$$

So, for $\mathbb{P}1$ finite element with ROCK2 time integration ($r = 2$ and $s = 1$), the parabolic approach is more efficient than the regularised elliptic one if $q > 3$ for problems in dimension $d = 2$ or if $q \geq 2$ for dimension $d = 3$.

Remark 6.1. *As the theoretical estimates show, the particular advantage of the parabolic approach (when compared to Ref. 24, 25) will be observed for three dimensional problems with large values for q. In particular, we expect the parabolic corrector to be particularly efficient in 3D, first because of* (51)*, second because of cost issues in relation with implementation. Indeed, while no matrix inversion is involved for solving the parabolic corrector problem in any dimension via explicit stabilised solvers (e.g. ROCK methods) this is not the case for the elliptic corrector problem. In 3D, even though the linear solver with $\mathcal{O}(N)$ complexity such as multigrid can be implemented, the prefactor will depend on the roughness of the conductivity tensor and the type of preconditioner used. However, in what follows we will concentrate on a 2D comparison as an exhaustive comparison with other approaches is not the aim of the paper.*

A comparison of the computational efficiency for the method described in the present paper and the regularised elliptic method of Ref. 24 is discussed below. We take $L = 2R/3$ and $T = \sqrt{\frac{1}{4\pi^2 \alpha\beta}}\,|R - L|$ (see (40)) for the parabolic case, and $L = 2R/3$ and $T = L^2(\log L)^{-4}$ (as in Ref. 24) for the regularised elliptic case. In the plots of Figure 7, the elapsed real times spent to solve the parabolic equation (9) and the regularised elliptic equation (45) are plotted against the corresponding error. We consider the coefficients (43) and discretized the cell problem in space with $\mathbb{P}1$ finite elements on a triangular mesh of size h. The time integration for the parabolic problem is performed by the ROCK2 method with adaptive time stepping. So, the time integration scheme is fed with an absolute tolerance, $atol$, and a relative tolerance, $rtol$, instead of a fixed time discretization Δt. In our computations, we took $atol = rtol = tol$. It is also

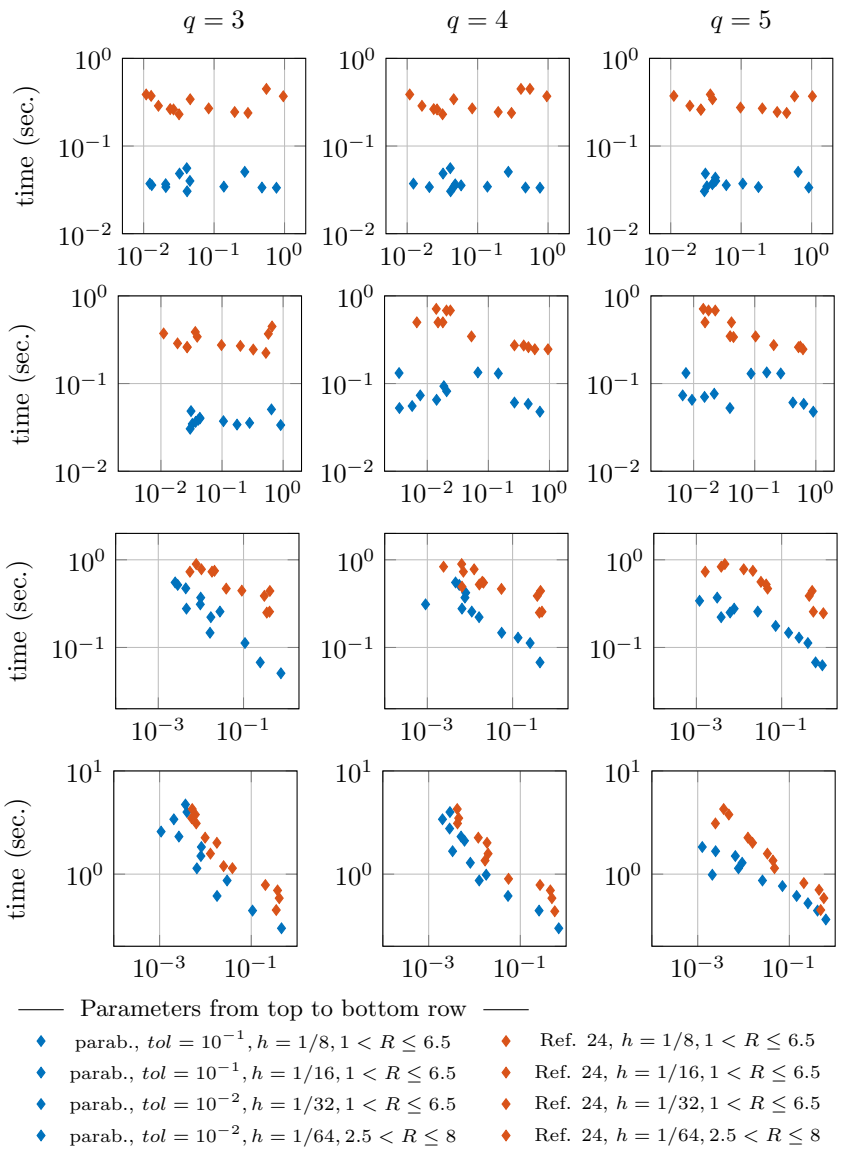


Figure 7: Comparison of the elapsed times (y-axis) against the approximation error (39) (x-axis) for two homogenization approaches.

worth mentioning that h and tol have to be refined concurrently to avoid error saturation due to too coarse discretizations in time or space. The tests were run for different choices of discretization and modelling parameters on a machine with 2 processors running at 2.6 GHz, with 14 cores each. The value of q varies along the rows, while the discretization parameters (h and tol) vary along the columns. In each plot, we depict the error and elapsed computation time for increasing values of R. In the first three rows $R \in [1, 6.5]$, while $R \in [2.5, 8]$ for the last one. The motivation for choosing R in such ranges is the following: for coarse discretizations and large sampling domains, the discretization error is dominating thus undermining the property of high convergence of the methods. The threshold $R \approx 6.5$, in the three coarser tests, has been empirically determined as the maximum domain size for which the discretization error does not exceed the resonance one. For the same reason, we excluded the values $R < 2$ from the finest computations, because for $R < 2$ the homogenized limit can be approximated more efficiently with coarser discretizations.

The plots of Figure 7 show that, for coarse values of tolerance tol, the parabolic method can reach the same error as the regularised one with less computational effort. In the two coarsest experiments ($h = 1/8$, $tol = 10^{-1}$ and $h = 1/16$, $tol = 10^{-1}$) the computational cost only slightly grows with increasing R, meaning that the elapsed time is dominated by overhead rather than actual computation. In the third row ($h = 1/32$, $tol = 10^{-2}$), the growth of the computational cost is shown more clearly and the computational time for the parabolic method is always shorter than for the elliptic method, in particular for higher order filters. Such a positive effect of using high order filters is visible also in the last row ($h = 1/64$, $tol = 10^{-2}$ and $q = 5$).

In conclusion, the use of high order filers is beneficial for the parabolic case, as it allows to rapidly achieve high accuracy approximations with relatively low computational cost.

7 Conclusion

In this work, we propose a novel approach for numerical homogenization, based on the solution of parabolic cell problems. We rigorously prove, by estimates of the fundamental solution, an arbitrary convergence rate for the resonance error in the periodic setting, but numerical tests demonstrate the same rates also for the boundary error in a non-periodic case. If filters of high order are used, the computation of the parabolic solutions by means of stabilised explicit solvers is asymptotically more efficient than the inversion of the discretized elliptic operator, required by elliptic approaches.

A Proof of Lemma 4.5

Lemma A.1. *Let $G(\mathbf{x}, t; \mathbf{y})$ be the fundamental solution (29) in $K_R \times (0, +\infty)$ for coefficients $a(\cdot) \in \mathcal{M}(\alpha, \beta, K_R)$. Recall that $\Delta = K_R \setminus R_{\tilde{R}}$, where $\tilde{R}$ is given*

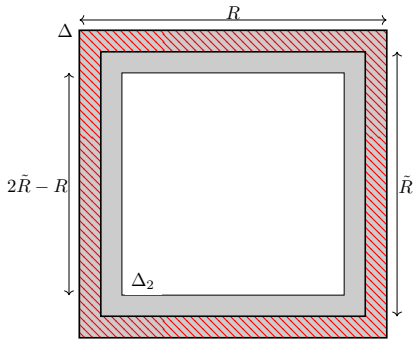


Figure 8: The boundary layers Δ and Δ_2.

in Definition 4.1. *Let* $\Delta_2 := K_R \setminus K_{2\tilde{R}-R}$ *and* $\mathbf{y} \in K_R$ *such that dist* $(\mathbf{y}, \Delta_2) \geq \epsilon$ *for arbitrarily small* $\epsilon > 0$. *Then, there exist a constant* $M > 0$ *such that*

$$\|\nabla G(\cdot, \cdot; \mathbf{y})\|_{L^2((0,T)\times\Delta)} \leq \frac{2M\beta}{\alpha} \|G(\cdot, \cdot; \mathbf{y})\|_{L^2((0,T)\times\Delta_2)}.$$

Proof. This is essentially a Caccioppoli estimate. First of all, we notice that $\Delta \subset \Delta_2$. Let us consider the smooth function $\eta_\Delta \in C^\infty(\Delta_2)$ satisfying:

$$0 \leq \eta_\Delta \leq 1, \quad \eta_\Delta \equiv 1 \quad \text{in } \Delta, \quad \eta_\Delta = 0 \quad \text{in } \partial\Delta_2 \setminus \partial\Delta, \quad \text{and } |\nabla \eta_\Delta| \leq M. \tag{52}$$

Let us consider the weak form of the parabolic problem solved by the fundamental solution on $K_R \times (0, T)$ with $\phi := \eta_\Delta^2 G$ as a test function:

$$-\int_0^T \int_{\Delta_2} \partial_t G \phi \, d\mathbf{x} \, dt = \int_0^T \int_{\Delta_2} \nabla \phi \cdot a(\mathbf{x}) \nabla G \, d\mathbf{x} \, dt, \tag{53}$$

The identity above is true because $\phi = 0$ on $\partial\Delta_2$: indeed $G = 0$ on the outer boundary ∂K_R, while $\eta_\Delta = 0$ on the inner boundary $\partial\Delta_2 \setminus \partial\Delta$. Now, we bound from below the right-hand side of (53):

$$\begin{aligned}
&\int_0^T \int_{\Delta_2} \nabla \phi \cdot a(\mathbf{x}) \nabla G \, d\mathbf{x} \, dt \\
&= \int_0^T \int_{\Delta_2} \eta_\Delta^2 \nabla G \cdot a(\mathbf{x}) \nabla G \, d\mathbf{x} \, dt + \int_0^T \int_{\Delta_2} 2\eta_\Delta G \nabla \eta_\Delta \cdot a(\mathbf{x}) \nabla G \, d\mathbf{x} \, dt \qquad (54) \\
&\geq \alpha \int_0^T \int_{\Delta_2} \eta_\Delta^2 |\nabla G|^2 \, d\mathbf{x} \, dt + \int_0^T \int_{\Delta_2} 2\eta_\Delta G \nabla \eta_\Delta \cdot a(\mathbf{x}) \nabla G \, d\mathbf{x} \, dt.
\end{aligned}$$

The last term can be bounded by Hölder and Young inequalities:

$$\int_0^T \int_{\Delta_2} 2\eta_\Delta G \nabla \eta_\Delta \cdot a(\mathbf{x}) \nabla G \, d\mathbf{x} \, dt \geq -2\beta \int_0^T \int_{\Delta_2} |\eta_\Delta G \nabla \eta_\Delta \cdot \nabla G| \, d\mathbf{x} \, dt$$

$$\geq -\frac{\alpha}{2}\int_0^T\int_{\Delta_2}\eta_\Delta^2\,|\nabla G|^2\,d\mathbf{x}\,dt-\frac{2\beta^2}{\alpha}\int_0^T\int_{\Delta_2}|\nabla\eta_\Delta|^2\,G^2\,d\mathbf{x}\,dt.$$

Hence, (54) becomes

$$\int_0^T\int_{\Delta_2}\nabla\phi\cdot a(\mathbf{x})\nabla G\,d\mathbf{x}\,dt \geq \frac{\alpha}{2}\int_0^T\int_{\Delta_2}\eta_\Delta^2\,|\nabla G|^2\,d\mathbf{x}\,dt-\frac{2\beta^2M^2}{\alpha}\int_0^T\int_{\Delta_2}G^2\,d\mathbf{x}\,dt. \quad (55)$$

We now bound from above the left-hand side of (53):

$$-\int_0^T\int_{\Delta_2}\partial_t G\phi\,d\mathbf{x}\,dt=-\int_0^T\int_{\Delta_2}\frac{1}{2}\frac{d}{dt}\left(G^2\eta_\Delta^2\right)\,d\mathbf{x}\,dt$$
$$=\frac{1}{2}\int_{\Delta_2}\underbrace{|G(\mathbf{x},0;\mathbf{y})|^2}_{=0,\text{ since }|x-y|>0.}\,|\eta_\Delta|^2\,d\mathbf{x}-\frac{1}{2}\int_{\Delta_2}|G(\mathbf{x},T;\mathbf{y})|^2\,|\eta_\Delta|^2\,d\mathbf{x}\leq 0 \quad (56)$$

Therefore, from (52), (53), (55) and (56), we conclude that

$$\int_0^T\int_{\Delta}|\nabla G|^2\,d\mathbf{x}\,dt\leq\int_0^T\int_{\Delta_2}\eta_\Delta^2\,|\nabla G|^2\,d\mathbf{x}\,dt\leq\left(\frac{2M\beta}{\alpha}\right)^2\int_0^T\int_{\Delta_2}G^2\,d\mathbf{x}\,dt.$$

□

Lemma 4.5. From (32) and from the symmetry of the fundamental solution, $G(\mathbf{x},t;\mathbf{y})=G(\mathbf{y},t;\mathbf{x})$, we estimate

$$\left|\theta^i(\mathbf{x},t)\right|\leq\|G(\cdot,t;\mathbf{x})\|_{L^2(\Delta)}\,\|\nabla\cdot(a(\cdot)\mathbf{e}_i)\|_{L^2(\Delta)} + C_\rho\beta\,\|G(\cdot,\cdot;\mathbf{x})\|_{L^2((0,t)\times\Delta)}\left\|\nabla v^i\right\|_{L^2((0,t)\times\Delta)} + C_\rho\beta\,\|\nabla G(\cdot,\cdot;\mathbf{x})\|_{L^2((0,t)\times\Delta)}\left\|v^i\right\|_{L^2((0,t)\times\Delta)}, \quad (57)$$

where C_ρ is an upper bound for the gradient of the cut-off function, $\nabla\rho$, of Definition 4.2.

Let us now consider a covering of Δ, defined as $\Delta_K:=\bigcup_{\mathbf{y}\in\partial K_{\frac{R+\tilde{R}}{2}}}K+\mathbf{y}$. Then, $|\Delta_K|=c(d)\left|\partial K_{\frac{R+\tilde{R}}{2}}\right|\operatorname{diam}(K)\leq CR^{d-1}$. By exploiting the periodic structure of v^i we have that, for each $t>0$,

$$\left\|v^i(\cdot,t)\right\|_{L^2(\Delta)}\leq\left\|v^i(\cdot,t)\right\|_{L^2(\Delta_K)}\leq\left(\frac{|\Delta_K|}{|K|}\right)^{1/2}\left\|v^i(\cdot,t)\right\|_{L^2(K)},$$
$$\left\|\nabla v^i(\cdot,t)\right\|_{L^2(\Delta)}\leq\left\|\nabla v^i(\cdot,t)\right\|_{L^2(\Delta_K)}\leq\left(\frac{|\Delta_K|}{|K|}\right)^{1/2}\left\|\nabla v^i(\cdot,t)\right\|_{L^2(K)}.$$

Thus, it is sufficient to bound $\left\|v^i(\cdot,t)\right\|_{L^2(K)}$ and $\left\|\nabla v^i(\cdot,t)\right\|_{L^2(K)}$ in the periodic cell to derive corresponding estimates on Δ. From standard energy estimates[5] and the Poincaré-Wirtinger inequality in the space $W^1_{per}(K)$, it is easy to see that

$$\|\nabla\cdot(a(\cdot)\mathbf{e}_i)\|_{L^2(\Delta)} \leq \left(\frac{|\Delta_K|}{|K|}\right)^{1/2} \|\nabla\cdot(a(\cdot)\mathbf{e}_i)\|_{L^2(K)}\,, \tag{58a}$$

$$\begin{aligned}\left\|\nabla v^i\right\|_{L^2((0,t)\times\Delta)} &\leq \left(\frac{|\Delta_K|}{|K|}\right)^{1/2} \left\|\nabla v^i\right\|_{L^2((0,t)\times K)} \\ &\leq \left(\frac{|\Delta_K|}{|K|}\right)^{1/2} \frac{1}{\sqrt{2\alpha}} \|\nabla\cdot(a(\cdot)\mathbf{e}_i)\|_{L^2(K)}\,,\end{aligned} \tag{58b}$$

$$\begin{aligned}\left\|v^i\right\|_{L^2((0,t)\times\Delta)} &\leq \left(\frac{|\Delta_K|}{|K|}\right)^{1/2} \left\|v^i\right\|_{L^2((0,t)\times K)} \\ &\leq \left(\frac{|\Delta_K|}{|K|}\right)^{1/2} \frac{C_P}{\sqrt{2\alpha}} \|\nabla\cdot(a(\cdot)\mathbf{e}_i)\|_{L^2(K)}\,,\end{aligned} \tag{58c}$$

where the Poincaré-Wirtinger constant C_P is independent of R.

Let us now consider two arbitrary constants b, c such that $b \geq \frac{|R-L|}{\left|2\tilde{R}-R-L\right|}$ and $0 < c \leq \nu\frac{\left|2\tilde{R}-R-L\right|^2}{|R-L|^2}$ (since $L < R-2$, we know that $2\tilde{R}-R-L > 0$). Then,

$$\begin{aligned}\frac{1}{\left|\tilde{R}-L\right|} \leq \frac{1}{\left|2\tilde{R}-R-L\right|} \leq \frac{b}{|R-L|}, \quad \text{and} \\ e^{-\nu\frac{|\tilde{R}-L|^2}{t}} \leq e^{-\nu\frac{|2\tilde{R}-R-L|^2}{t}} \leq e^{-c\frac{|R-L|^2}{t}},\end{aligned} \tag{59}$$

where ν is the constant in (30) and $t > 0$.By using (30), the first term in (57) is estimated as

$$\begin{aligned}\|G(\cdot,t;\mathbf{x})\|_{L^2(\Delta)} &\leq \left[\int_\Delta \frac{C^2}{t^d} e^{-2\nu\frac{|\mathbf{x}-\mathbf{y}|^2}{t}}\,d\mathbf{y}\right]^{\frac{1}{2}} \\ &\leq \frac{C\,|\Delta|^{1/2}}{t^{d/2}} e^{-\nu\frac{|\tilde{R}-L|^2}{t}} \leq \frac{C\,|\Delta|^{1/2}}{t^{d/2}} e^{-c\frac{|R-L|^2}{t}},\end{aligned} \tag{60}$$

since $|\mathbf{x}-\mathbf{y}| \geq \left|\tilde{R}-L\right|$ for $\mathbf{x} \in K_L$ and $\mathbf{y} \in \Delta$, and thanks to (59). Likewise, the $L^2\left((0,t)\times\Delta\right)$-norm of the fundamental solution is bounded by

$$\|G(\cdot,\cdot;\mathbf{x})\|_{L^2((0,t)\times\Delta)} \leq C\,|\Delta|^{1/2}\left[\int_0^t \frac{1}{s^d} e^{-2\nu\frac{|\tilde{R}-L|^2}{s}}\,ds\right]^{\frac{1}{2}}.$$

[5] By testing the solution v^i against itself, we know that $\frac{1}{2}\frac{d}{dt}\|v\|^2_{L^2(K)} + \alpha\|\nabla v\|^2_{L^2(K)} \leq 0$. Thus, $\left\|\nabla v^i\right\|^2_{L^2((0,+\infty)\times K)} \leq \frac{1}{2\alpha}\|v(\cdot,0)\|^2_{L^2(K)}$ by integration in time.

The time integral can be bounded in different ways, depending on the dimension d: If $d \leq 2$ it is straightforward to prove that

$$\int_0^t \frac{1}{s^d} e^{-2\nu \frac{|\tilde{R}-L|^2}{s}}\, ds \leq \frac{1}{2\nu \left|\tilde{R}-L\right|^2} t^{2-d} e^{-2\nu \frac{|\tilde{R}-L|^2}{t}},$$

while, when $d \geq 3$, the integral can be computed exactly[6] and it can be bounded as

$$\int_0^t \frac{1}{s^d} e^{-2\nu \frac{|\tilde{R}-L|^2}{s}}\, ds \leq \begin{cases} (d-2)! \left(\frac{1}{2\nu \left|\tilde{R}-L\right|^2}\right)^{d-1}, & \text{if } \frac{2\nu \left|\tilde{R}-L\right|^2}{t} \leq 1, \\ \frac{\kappa}{2\nu \left|\tilde{R}-L\right|^2} t^{2-d} e^{-2\nu \frac{|\tilde{R}-L|^2}{t}}, & \text{if } \frac{2\nu \left|\tilde{R}-L\right|^2}{t} > 1, \end{cases}$$

for some $\kappa > 0$. By assuming that $t \leq 2\nu \left|\tilde{R}-L\right|^2$ and by (59), one concludes that there exists $C > 0$, independent of R and L, such that:

$$\begin{aligned} \|G(\cdot,\cdot;\mathbf{x})\|_{L^2((0,t)\times\Delta)} &\leq \frac{C\,|\Delta|^{1/2}}{\sqrt{2\nu}\left|\tilde{R}-L\right|} \frac{1}{t^{d/2-1}} e^{-\nu \frac{|\tilde{R}-L|^2}{t}} \\ &\leq \frac{C\,|\Delta|^{1/2}\, b}{\sqrt{2\nu}\,|R-L|} \frac{1}{t^{d/2-1}} e^{-c \frac{|R-L|^2}{t}}. \end{aligned} \tag{61}$$

Finally, we use the result of Lemma A.1 and, again, (59) to bound the norm of the gradient:

$$\begin{aligned} \|\nabla G(\cdot,\cdot;\mathbf{x})\|_{L^2((0,t)\times\Delta)} &\leq \frac{2M\beta}{\alpha} \|G(\cdot,\cdot;\mathbf{x})\|_{L^2((0,t)\times\Delta_2)} \\ &\leq \frac{2M\beta}{\alpha} \frac{C\,|\Delta_2|^{1/2}}{\sqrt{2\nu}\left|2\tilde{R}-R-L\right|} \frac{1}{t^{d/2-1}} e^{-\nu \frac{|2\tilde{R}-R-L|^2}{t}} \\ &\leq \frac{2M\beta}{\alpha} \frac{C\,|\Delta_2|^{1/2}\, b}{\sqrt{2\nu}\,|R-L|} \frac{1}{t^{d/2-1}} e^{-c \frac{|R-L|^2}{t}}. \end{aligned} \tag{62}$$

Moreover, we know that $|\Delta| \leq |\Delta_K|$ and $|\Delta_2| \leq 2\,|\Delta_K|$. Thus, by plugging estimates (58) and (60)–(62) into (57), and by assuming that the periodic cell is the unit square, $|K| = 1$, one gets

$$\left|\theta^i(\mathbf{x},t)\right| \leq \frac{C\,|\Delta|^{1/2}}{t^{d/2}} e^{-c \frac{|R-L|^2}{t}} \left(\frac{|\Delta_K|}{|K|}\right)^{1/2} \|\nabla \cdot (a(\cdot)\mathbf{e}_i)\|_{L^2(K)}$$

[6] The function $F(s) = \left(\frac{1}{2\nu|\tilde{R}-L|^2}\right)^{d-1} \left[\sum_{k=0}^{d-2} \frac{(d-2)!}{k!} \left(2\nu \frac{\left|\tilde{R}-L\right|^2}{t}\right)^k\right] e^{-2\nu \frac{|\tilde{R}-L|^2}{t}}$ is the primitive of $f(s) = s^{-d} e^{-2\nu \frac{\left|\tilde{R}-L\right|^2}{s}}$.

$$
\begin{aligned}
&+ C_\rho\beta \frac{C\,|\Delta|^{1/2}\,b}{\sqrt{2\nu}\,|R-L|}\frac{1}{t^{d/2-1}} e^{-c\frac{|R-L|^2}{t}} \left(\frac{|\Delta_K|}{|K|}\right)^{1/2} \frac{1}{\sqrt{2\alpha}} \left\|\nabla\cdot(a(\cdot)\mathbf{e}_i)\right\|_{L^2(K)} \\
&+ C_\rho\beta \frac{2M\beta}{\alpha}\frac{C\,|\Delta_2|^{1/2}\,b}{\sqrt{2\nu}\,|R-L|}\frac{1}{t^{d/2-1}} e^{-c\frac{|R-L|^2}{t}} \left(\frac{|\Delta_K|}{|K|}\right)^{1/2} \frac{C_P}{\sqrt{2\alpha}} \left\|\nabla\cdot(a(\cdot)\mathbf{e}_i)\right\|_{L^2(K)} \\
&\leq \left[1 + C_\rho\beta\frac{bt}{\sqrt{2\nu}\,|R-L|}\frac{1}{\sqrt{2\alpha}} + C_\rho\beta\frac{2M\beta}{\alpha}\frac{\sqrt{2}bt}{\sqrt{2\nu}\,|R-L|}\frac{C_P}{\sqrt{2\alpha}}\right]\times \\
&\qquad\qquad \times \frac{C\,|\Delta_K|\,\left\|\nabla\cdot(a(\cdot)\mathbf{e}_i)\right\|_{L^2(K)}}{t^{d/2}} e^{-c\frac{|R-L|^2}{t}} \\
&\qquad\qquad \leq \left(1 + C_2\frac{t}{|R-L|}\right)\frac{C_1 R^{d-1}\left\|\nabla\cdot(a(\cdot)\mathbf{e}_i)\right\|_{L^2(K)}}{t^{d/2}} e^{-c\frac{|R-L|^2}{t}},
\end{aligned}
$$

with constants $C_1 > 0$ and $C_2 := \dfrac{C_\rho\beta b}{2\sqrt{\alpha\nu}}\left(1 + 2\sqrt{2}MC_P\dfrac{\beta}{\alpha}\right)$.

□

Acknowledgements

This work is partially supported by the Swiss National Science Foundation, grant No. 200020_172710.

References

1. Assyr Abdulle. Fourth order Chebyshev methods with recurrence relation. *SIAM J. Sci. Comput.*, 23(6):2041–2054, 2002.

2. Assyr Abdulle. On a priori error analysis of fully discrete heterogeneous multiscale FEM. *Multiscale Model. Simul.*, 4(2):447–459, 2005.

3. Assyr Abdulle. The finite element heterogeneous multiscale method: a computational strategy for multiscale PDEs. In *Multiple scales problems in biomathematics, mechanics, physics and numerics*, volume 31 of *GAKUTO Internat. Ser. Math. Sci. Appl.*, pages 133–181. Gakkōtosho, Tokyo, 2009.

4. Assyr Abdulle. A priori and a posteriori error analysis for numerical homogenization: a unified framework. *Ser. Contemp. Appl. Math. CAM*, 16:280–305, 2011.

5. Assyr Abdulle, Doghonay Arjmand, and Edoardo Paganoni. Exponential decay of the resonance error in numerical homogenization via parabolic and elliptic cell problems. *C. R. Math. Acad. Sci. Paris*, 357:545–551, 2019.

6. Assyr Abdulle, Weinan E, Björn Engquist, and Eric Vanden-Eijnden. The heterogeneous multiscale method. *Acta Numer.*, 21:1–87, 2012.

7. Assyr Abdulle and Alexei A. Medovikov. Second order Chebyshev methods based on orthogonal polynomials. *Numer. Math.*, 90(1):1–18, 2001.

8. Assyr Abdulle and Gilles Vilmart. Analysis of the finite element heterogeneous multiscale method for quasilinear elliptic homogenization problems. *Math. Comp.*, 83(286):513–536, 2014.

9. Doghonay Arjmand and Olof Runborg. A time dependent approach for removing the cell boundary error in elliptic homogenization problems. *J. Comput. Phys.*, 314(Supplement C):206–227, 2016.

10. Doghonay Arjmand and Olof Runborg. Estimates for the upscaling error in heterogeneous multiscale methods for wave propagation problems in locally-periodic media. ArXiv e-print 1605.02386, 2016.

11. Doghonay Arjmand and Olof Runborg. Estimates for the upscaling error in heterogeneous multiscale methods for wave propagation problems in locally periodic media. *Multiscale Model. Simul.*, 15(2):948–976, 2017.

12. Doghonay Arjmand and Christian Stohrer. A finite element heterogeneous multiscale method with improved control over the modeling error. *Communications in Mathematical Sciences*, 14(2):463–487, 2016.

13. Scott Armstrong, Tuomo Kuusi, and Jean-Christophe Mourrat. *Quantitative Stochastic Homogenization and Large-Scale Regularity.* Springer, 2019.

14. D. G. Aronson. Non-negative solutions of linear parabolic equations. *Ann. Sc. Norm. Super. Pisa Cl. Sci.*, Ser. 3, 22(4):607–694, 1968.

15. Alain Bensoussan, Jacques-Louis Lions, and George Papanicolaou. *Asymptotic analysis for periodic structures.* North-Holland Publishing Co., Amsterdam, 1978.

16. Xavier Blanc and Claude Le Bris. Improving on computation of homogenized coefficients in the periodic and quasi-periodic settings. *Netw. Heterog. Media*, 5(1):1–29, 2010.

17. Haim Brezis. *Functional analysis, Sobolev spaces and partial differential equations.* Springer Science & Business Media, 2010.

18. Doina Cioranescu and Patrizia Donato. *An introduction to homogenization*, volume 17 of *Oxford Lecture Series in Mathematics and its Applications.* Oxford University Press, New York, 1999.

19. Weinan E. *Principles of multiscale modeling.* Cambridge University Press, Cambridge, 2011.

20. Weinan E and Björn Engquist. The heterogeneous multiscale methods. *Commun. Math. Sci.*, 1(1):87–132, 2003.

21. Weinan E, Pingbing Ming, and Pingwen Zhang. Analysis of the heterogeneous multiscale method for elliptic homogenization problems. *J. Amer. Math. Soc.*, 18(1):121–156, 2005.

22. Lawrence C. Evans. *Partial differential equations*, volume 19 of *Graduate Studies in Mathematics*. American Mathematical Society, Providence, RI, second edition, 2010.

23. A. George and E. Ng. On the complexity of sparse QR and LU factorization of finite-element matrices. *SIAM J. Sci. and Stat. Comput.*, 9(5):849–861, 1988.

24. Antoine Gloria. Reduction of the resonance error. Part 1: Approximation of homogenized coefficients. *Math. Models Methods Appl. Sci.*, 21(8):1601–1630, 2011.

25. Antoine Gloria and Zakaria Habibi. Reduction in the resonance error in numerical homogenization ii: Correctors and extrapolation. *Found. Comput. Math.*, 16(1):217–296, Feb 2016.

26. Antoine Gloria, Stefan Neukamm, and Felix Otto. Quantification of ergodicity in stochastic homogenization: optimal bounds via spectral gap on Glauber dynamics. *Inventiones mathematicae*, 199(2):455–515, 2015.

27. Antoine Gloria and Felix Otto. The corrector in stochastic homogenization: optimal rates, stochastic integrability, and fluctuations. arXiv:1510.08290.

28. Antoine Gloria and Felix Otto. An optimal variance estimate in stochastic homogenization of discrete elliptic equations. *Ann. Probab.*, 39(3):779–856, 05 2011.

29. Antoine Gloria and Felix Otto. An optimal error estimate in stochastic homogenization of discrete elliptic equations. *Ann. Appl. Probab.*, 22(1):1–28, 02 2012.

30. Patrick Henning and Axel Målqvist. Localized orthogonal decomposition techniques for boundary value problems. *SIAM J. Sci. Comput.*, 36(4):A1609–A1634, 2014.

31. Thomas Y. Hou and Xiao-Hui Wu. A multiscale finite element method for elliptic problems in composite materials and porous media. *J. Comput. Phys.*, 134(1):169–189, 1997.

32. Thomas Y. Hou, Xiao-Hui Wu, and Zhiqiang Cai. Convergence of a multiscale finite element method for elliptic problems with rapidly oscillating coefficients. *Math. Comp.*, 68(227):913–943, 1999.

33. Thomas J.R. Hughes, Gonzalo R. Feijóo, Luca Mazzei, and Jean-Baptiste Quincy. The variational multiscale method – a paradigm for computational mechanics. *Comput. Methods Appl. Mech. Engrg.*, 166(1):3 – 24, 1998. Advances in Stabilized Methods in Computational Mechanics.

34. Vasilii V. Jikov, Sergei M. Kozlov, and Olga A. Oleinik. *Homogenization of differential operators and integral functionals*. Springer-Verlag, Berlin, Heidelberg, 1994.

35. Ioannis G. Kevrekidis, C. William Gear, James M. Hyman, Panagiotis G. Kevrekidis, Olof Runborg, and Constantinos Theodoropoulos. Equation-free, coarse-grained multiscale computation: enabling microscopic simulators to perform system-level analysis. *Commun. Math. Sci.*, 1(4):715–762, 2003.

36. Jacques-Louis Lions and Enrico Magenes. *Problèmes aux limites non homogènes et applications*, volume 1 of *Travaux et recherches mathématiques*. Dunod, Paris, 1968.

37. Axel Målqvist and Daniel Peterseim. Localization of elliptic multiscale problems. *Math. Comp.*, 83(290):2583–2603, 2014.

38. Jean-Christophe Mourrat. Efficient methods for the estimation of homogenized coefficients. *Found. Comput. Math.*, 19(2):435–483, Apr 2019.

39. L. E. Payne and H. F. Weinberger. An optimal Poincaré inequality for convex domains. *Arch. Rational Mech. Anal.*, 5:286–292, 1960.

40. Yousef Saad. *Iterative methods for sparse linear systems*, volume 82. SIAM, 2003.

41. S Spagnolo. Sulla convergenza di soluzioni di equazioni paraboliche ed ellittiche. *Ann. Sc. Norm. Super. Pisa Cl. Sci.*, 22(4):571–597, 1968.

42. Pieter van der Houwen and Ben P. Sommeijer. On the internal stage Runge-Kutta methods for large m-values. *Z. Angew. Math. Mech.*, 60:479–485, 1980.

43. Xingye Yue and Weinan E. The local microscale problem in the multiscale modeling of strongly heterogeneous media: effects of boundary conditions and cell size. *J. Comput. Phys.*, 222(2):556–572, 2007.